Chemical Bonding Effects in the Oxygen $K\alpha$ X-Ray Emission Bands of Silica

T. L. Gilbert* and W. J. Stevens*†
Argonne National Laboratory, Argonne, Illinois 60439

H. Schrenk,‡ M. Yoshimine, and P. S. Bagus
IBM Research Laboratory, San Jose, California 95114

(Received 30 November 1972)

Self-consistent-field (SCF) atomic and molecular orbitals and energy levels for O, SiO, and collinear Si_2O are used to interpret the oxygen $K\alpha$ soft-x-ray emission spectrum of silica. The O and Si_2O orbitals are calculated in both the frozen-orbital (FO) and relaxed-orbital (RO) approximations. The results are used to calculate the emission-line energies and oscillator strengths for the oxygen $K\alpha$ spectrum of each species. The calculated separation between the π and σ emission lines of collinear Si_2O in both the RO approximation (6.9 eV) and the FO approximation (6 eV) are somewhat larger than the observed separation between the principal emission peak and low-energy satellite in silica (5 eV), but it is shown that the bending of the Si-O-Si bond in silica will reduce the separation. The calculated position of the principal line for Si_2O (525.7 eV in the RO approximation) is in good agreement with the principal peak observed in silica (526 eV). The $3p$ and $3s$ atomic orbitals of silicon are found to be strongly modified from their free-atom shape in both SiO and Si_2O; enough to make an order-of-magnitude difference between oscillator strengths calculated in the SCF and linear-combination-of-atomic-orbitals approximations. The modifications of the oxygen valence orbitals are relatively small. The oxygen sp hybridization is quite small. The atomic population of the 5σ(SiO) level is 88% $2s$(O), 2% $2p$(O), 4% $3p$(Si) and 5% $3s$(Si). The d hybridization is also small: a maximum of 5% $3d$(Si) in the $2\pi_u(Si_2O)$ level and 1% $3d$(O) in the $2\pi_g(Si_2O)$ level. Crossover transitions in a literal sense are negligible. The $2s$(O) line in the silicon $K\beta$ spectrum of SiO, for example, [the 5σ(SiO) $\rightarrow 1\sigma$(SiO) transition], is almost entirely a vertical transition which comes from the small $3p$(Si) admixture. An atomic population analysis gives ionicities of $Si^{+0.78}O^{-0.78}$ and $Si_2^{+0.37}O^{-0.74}$

I. INTRODUCTION

Within the past few years there have been a number of experimental studies of the satellite structure of the oxygen $K\alpha$ emission band in silica. There have also been a number of semiempirical calculations of the corresponding energy spectra for molecular fragments. These calculations leave several questions of interpretation unanswered. The work reported herein was undertaken to resolve these questions and to demonstrate the manner in which *ab initio* calculations on molecular fragments can be used to provide a more reliable and detailed interpretation of soft-x-ray emission spectra in solids.

The experimental data are summarized in Fig. 1. Emission spectra from several sources, taken from published figures, have been plotted together after scaling to equal peak heights and matching abscissas. The errors introduced by replotting from journal illustrations do not appear to be large enough to cause any serious loss in the experimental information. The closest correspondence is between the measurements of Fischer[1] and of Klein and Chun.[2] We take this as an indication that these are the most reliable data. Both find a principal peak at 526 eV, a satellite very close to 521 eV, and a slight shoulder on the low-energy side of the principal peak suggesting the existence of an unresolved satellite between 1 and 2 eV below the peak.

The data of Mattson and Ehlert[3] show the same features, but the positions are displayed about 0.5 eV to higher energies. They also observe some high-energy satellites. These satellites are, however, strongly dependent on the material used for the dispersing element of the x-ray spectrometer and the manner of excitation, so that it would be fruitless to attempt to interpret them from the available data.[4] Multiple-ionization effects also complicate the interpretation of high-energy satellites.

The data of Ershov and Lukirskii[5] show the same two primary features, but the principal peak is at 525 eV and the secondary peak is at 519 eV. There is no evidence of a low-energy shoulder on the principal peak, but there is a small shoulder at 514 eV. This is probably spurious, for there is no evidence of such a shoulder in the data of Klein and Chun, and Fischer states that he has looked carefully for such a peak and found no evidence for it.[6] Ershov and Lukirskii also show an indication of a small shoulder on the high-energy side of the principal peak, but the comments in the preceding paragraph concerning high-energy satellites apply here also.

The ratio of the height of the principal peak to the height of the low-energy satellite is approximately 4:1 for all four sets of data. When the

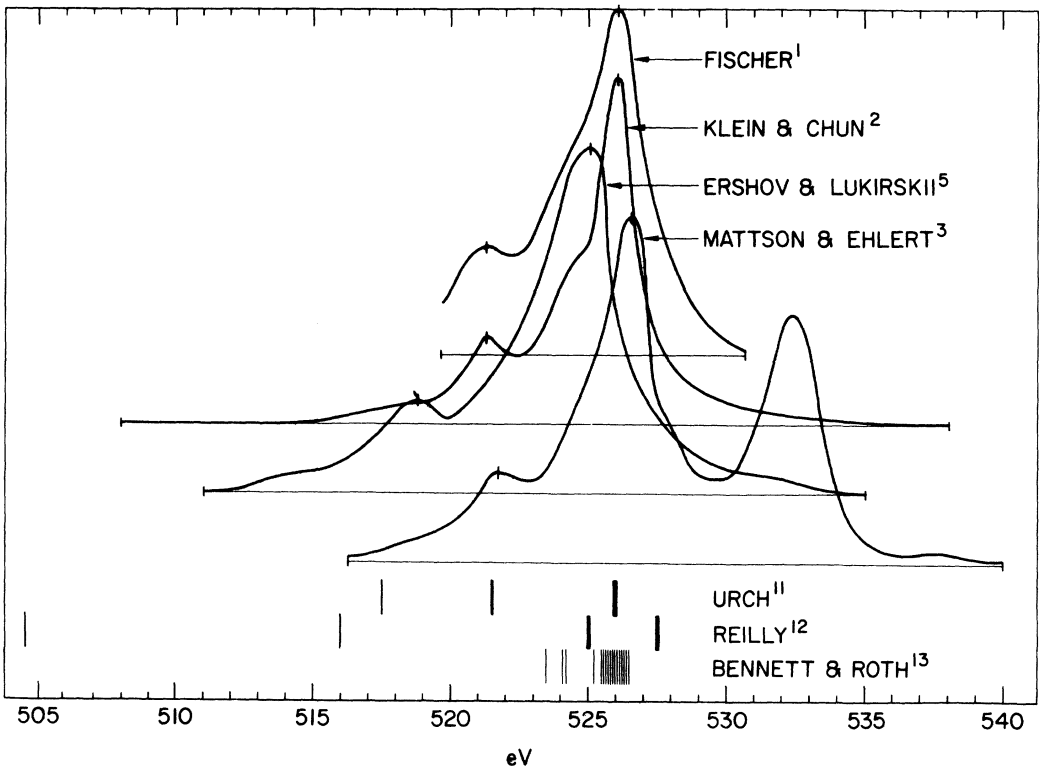

FIG. 1. Summary of observed oxygen $K\alpha$ x-ray emission spectra in silica and the results of previous semiempirical calculations.

broader base of the principal peak is taken into account, one may crudely estimate the ratio of the integrated intensities to be of the order of 8:1, within liberal limits of uncertainty. This figure is probably an upper limit, for it does not appear that the base of the principal peak is more than twice that of the satellite, and it may be less.

It is of interest to contrast the soft-x-ray emission spectra with photoemission spectra obtained by electron spectroscopy.[7] Although electron spectroscopy provides higher instrumental resolution, the soft-x-ray emission spectra provide more information. The former involve electronic transitions from valence to the continuum levels and hence provide a fairly uniform sampling of the charge density of the valence levels throughout the crystal. The latter involve electronic transitions from the valence levels to a core level and hence provide a measure of the charge density of the valence levels in the vicinity of the nucleus of a given atomic species. These can be quite different, as can be seen by comparing the silicon $K\beta$ and oxygen $K\alpha$ emission spectra in silica.[2,5] [One of the more interesting contrasts is the presence of a $2s$(O) line in the silicon $K\beta$ spectrum but not in the oxygen $K\alpha$ spectrum, a matter which will be discussed in more detail later.] The photoemission spectrum of SiO_2 has been measured by DiStefano and Eastman[8] using both ultraviolet and x-ray excitation. The structure is consistent with what one might expect from combining the $OK\alpha$ and $SiK\beta$ soft-x-ray emission spectra.

A qualitative interpretation of these data is evident from the geometry of silica. There are 13 known forms of silica, of which all but one (stishovite) consist of arrays of SiO_4 tetrahedra linked together by shared oxygen atoms at each vertex in the manner shown in Fig. 2. The bond lengths and bond angles differ slightly in the different lattice

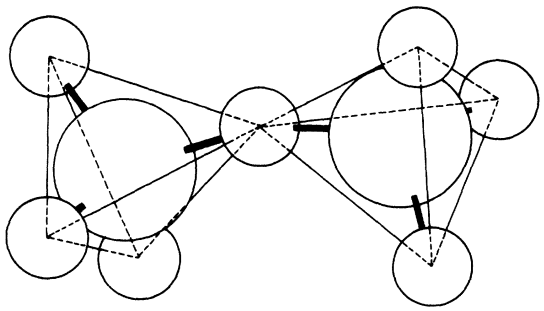

FIG. 2. Linked SiO_4 tetrahedral units in silica. The large atoms are silicon, the small ones oxygen.

arrangements, but the local geometry of the tetrahedral units and their coupling ramains the same in the absence of defects. [The Si-O bond length varies from 1.52 to 1.69 Å [2.9 to 3.3 B, where 1 B (bohr) = 0.52918 Å] with a mean of 1.612 Å (3.046 B), and the Si-O-Si bond angle varies from 120° to 150°.[9] In vitreous silica there is a distribution of angles with a maximum at about 144°.[10]] We can expect that the dominant features of the oxygen $K\alpha$ spectrum (the principal peak and low-energy satellite) will be reproduced by a model consisting of a collinear Si-O-Si fragment. In this model the $2p$ valence electrons of oxygen may be separated into two groups: two σ electrons and four π electrons. The σ electrons will be more strongly bonded than the π electrons, so that they will have a lower orbital energy. Hence, we may expect a spectrum with two peaks: a principal peak from the $2p\pi$ electrons dropping down to the oxygen $1s$ level, and a somewhat smaller peak at lower energies from $2p\sigma$ electrons dropping down to the oxygen $1s$ level. Bending of the bond may explain the shoulder on the low-energy side of the principal peak, and coupling with more distant neighbors will broaden the emission lines of Si_2O into bands, but the dominant features should not be affected.

This reasoning is so simple and straightforward that it would be difficult not to accept the validity of such a model. But calculations are still needed in order to verify it and to provide a more detailed picture of the electronic structure. The calculations which have been published to data have been semiempirical. The oxygen $K\alpha$ spectra inferred from these calculations are summarized at the bottom of Fig. 1.

A very simple Hückel calculation based on an SiO_4 tetrahedral fragment has been published by Urch.[11] Using intuitive semiempirical arguments, Urch inferred that the spectrum should consist of a broad intense band corresponding to electrons dropping from $2p$ lone pairs or π orbitals into the oxygen $1s$ orbital, a somewhat less intense peak about 4 eV lower, and a still weaker peak another 4 eV lower. This interpretation is not conclusive. The parametrization is highly simplified; arbitrary correction factors are introduced; and an SiO_4 fragment does not take into account the influence of the second Si-O bond linking each oxygen atom. The rather large oxygen sp hybridization is also open to question. The lowest satellite corresponds to an electron dropping from a hybridized oxygen $2s$ level into a $1s$ level. The experimental evidence (noted above) and symmetry considerations (see below) indicate that this satellite would not be observable.

A simplified linear-combination-of-atomic-orbitals to give molecular orbitals (LCAO-MO) treatment of an Si-O-Si fragment, using sp^3 hybrids for the silicon orbitals, has been reported by Reilly.[12] The oxygen hybrids were constructed in such a manner that the sp mixing was determined by the Si-O-Si bond angle rather than by matrix elements coupling the s and p orbitals. The original oxygen $2s$ level splits in a roughly symmetrical manner into two levels, both with strong $2p$ components. Reilly obtains a dominant band associated with the lone pairs, one satellite about 10 eV below this band, and another satellite about 10 eV below the first one. Qualitatively, Reilly and Urch predict the same satellite structure, but their predicted separations differ by a factor of about $2\frac{1}{2}$. The *ad hoc* procedure used by Reilly to calculate the mixing, and the large mixing of the oxygen $2s$ and $2p$ orbitals, are open to question.

Bennett and Roth[13] have published extended Hückel-method calculations for somewhat larger fragments. The chief difference between their calculations and those of Urch and of Reilly is that extended Hückel theory is used in a straightforward and consistent manner. Their level separations are much smaller. They obtain, for both an eight-molecule β-crystobalite structure (where a "molecule" is an SiO_2 fragment) and an idealized eight-molecule structure in which the Si-O-Si fragments are collinear, about 18 levels near the oxygen $2p$ level. These levels may be grouped into a very broad band and two weak satellites. However, the separation between the principal band and the satellites is of order of 1 eV, which is comparable to or less than the width of the primary peak.

More sophisticated calculations have been published recently by Collins, Cruickshank, and Breeze[14] for the silicate ion and orthosilicic acid, and used to interpret the silicon $L_{2,3}$ x-ray emission spectrum. These calculations cannot, unfortunately, be used to interpret the oxygen $K\alpha$ emission spectrum in silica because the second Si-O bond associated with each oxygen atom provides a rather different chemical environment.

A list of other related contributions to the measurement and interpretation of soft-x-ray emission spectra in insulating materials would include the work of Fischer on titanium, vanadium, and chromium oxides and also some nitrides and carbides[15]; the work of Glen and Dodd on glasses[16]; and the work of Koster on a number of oxides and fluorides.[17] Ruffa's semiempirical valence-bond calculations should also be mentioned.[18] A more complete list of references may be found in the review articles by Nagel[19] and by Baun and Fisher,[20] and in the proceedings of the Strathclyde conference.[21]

The three semiempirical calculations discussed above are in rather marked disagreement with each other and also with experimental observations. This disagreement, plus the fact that a

semiempirical calculation with adjustable parameters does not provide convincing justification for a model used to interpret two emission lines, leaves us roughly where we were at the start—with a very plausible model that we are inclined to accept on faith, but no independent verification. In this situation one may turn to *ab initio* calculations.

The *ab initio* calculations presented herein will still be model calculations. The effect of nuclear motion is omitted by assuming that the positions of the nuclei are fixed, and the effect of all but nearest neighbors is neglected by using molecular fragments. These neglected effects could be included, but they would require much more elaborate calculations of adiabatic potential surfaces for the fragments, Franck-Condon factors, and the electronic energy bands. We are, by implication, assuming that nuclear motion and distant neighbors merely introduce broadening without greatly affecting the positions or integrated intensities of the dominant peaks. Regardless of whether this assumption should eventually prove to be valid, we argue that one should investigate local interactions, which will have a strong effect on the peak positions and integrated intensities, before undertaking the much more elaborate calculations required in order to reproduce the entire spectral distribution of an emission band.

Systematic mathematical approximations will also be introduced, viz., the single-configuration self-consistent-field approximation and the Roothaan-expansion method. However, once the initial model and mathematical approximations have been chosen, no adjustable parameters are allowed. Since the approximations are well defined and have been used for a variety of calculations on atoms and small molecules, we have some *a priori* knowledge of their limits of validity and the magnitude of the errors. We can, therefore, make tentative use of the wave function to predict and interpret some of the more subtle details of the electronic structure. At the very least, the systematic nature of the *ab initio* approach enables us to assess where we stand and what improvements in the model will be needed in order to reach an acceptable level of accurate calculations for interpreting and predicting observed phenomena. This is the rationale for undertaking the calculations reported herein.

The use of an Si_2O model, which is central to our approach, merits some further discussion. It implies that the oxygen-oxygen interaction is a relatively small effect which can be neglected as a first approximation. This is at variance with models used to interpret the polarizibility of silica, which picture the silicon atoms as small nonoverlapping positive ions and the oxygen atoms as large strongly overlapping negative ions.[22] In Fig. 2 we show the silicon atoms as approximately twice the size of the oxygen atoms. This is consistent with the average Hartree-Fock radii of the valence orbitals[23,24] ($\langle r\rangle_{3p(Si)} = 2.75$ B, $\langle r\rangle_{3s(Si)} = 2.21$ B, $\langle r\rangle_{2p(O)} = 1.23$ B, and $\langle r\rangle_{2s(O)} = 1.14$ B) and also the tetrahedral covalent radii of Pauling,[25] ($R_{Si} = 2.21$ B and $R_O = 1.25$ B). We note, however, that the valence orbitals of silicon are rather diffuse. (See Fig. 3.) This suggests that one might draw the radii in such a manner that the valence electrons of silicon lie largely within the volume occupied by the oxygen atom, leading to a picture of small Si^{+4} ions surrounded by large O^{--} ions. However, the silicon valence orbitals are still centered on the silicon nuclei rather than the oxygen nuclei, so that this does not appear to us to be a natural interpretation. If the ionic picture were valid, then it would be reflected in the atomic population analysis of the self-consistent-field molecular orbitals (SCF-MO's). The oxygen atomic orbital components would be significantly larger than the separated-atom orbitals, and a large charge transfer from the silicon to the oxygen atomic orbital components would occur. In fact, we find that the oxygen atomic orbital components are nearly the same as for the separated-atom orbitals (there is a somewhat larger change in the silicon orbitals, but it does not support a strongly ionic picture), and

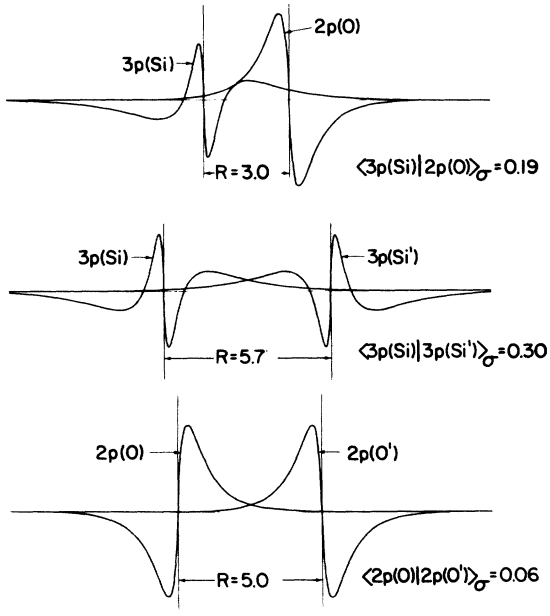

FIG. 3. Orbital amplitudes and overlaps for the unmodified $p\sigma$ valence orbitals of silicon and oxygen. [Note that the radial component of the *local* amplitude, $R_{nl}(r) = r^{-1}P_{nl}(r)$, rather than the radial amplitude, $P_{nl}(r)$, has been plotted. The normalization is $\int_0^\infty R_{nl}^2(r)r^2\,dr = \int_0^\infty P_{nl}^2(r)\,dr = 1$].

the charge transfer is represented by the formulas $Si^{+0.78}O^{-0.78}$ and $Si_2^{+0.37}O^{-0.74}$. We anticipate that the oxygen charge in Si_2O_7 (and silica) will be smaller, perhaps of the order of $Si^{+}O_2^{-0.5}$; certainly not anything close to $Si^{+4}O_2^{-2}$.

If one adopts the viewpoint suggested by an atomic population analysis of SCF-MO's, and uses the valence orbital overlaps as a measure of the covalent interatomic interactions, then the Si-O interaction is very strong (much stronger than the overlap of 0.19 would indicate, since the overlap is so large that there are appreciable regions of negative overlap density which partially cancel the regions of positive overlap density), the Si-Si interaction is also quite strong, but the O-O interaction is rather weak. (See Fig. 3.) From this viewpoint an Si_2O model, which includes the Si-O and Si-Si interactions but neglects the O-O interactions, is a reasonable one.

A calculation of the $K\alpha$ emission line for atomic oxygen is presented in Sec. II. One purpose of this calculation is to provide a reference calculation for a rough calibration of the errors in the calculated line positions. It demonstrates the importance of hole polarization, and also the fact that one can prove very little from qualitative agreement between observed and calculated spectra. The multiplet structure of atomic oxygen gives rise to an emission spectrum which is in as good agreement with the observed emission spectrum for oxygen in silica as some of the semiempirical calculations noted above. A more rigorous calculation is, therefore, needed in order to verify our belief that the observed structure is due to chemical bonding effects.

A calculation of the $K\alpha$ emission line for oxygen in the diatomic molecule SiO is presented in Sec. III. Although an SiO fragment is not a good model for quantitative studies of the oxygen emission spectrum in silica because it omits the second bond, it provides a simple and useful model for investigating certain qualitative features of the $OK\alpha$ emission spectrum. In particular, it is useful as a limiting model for examining the oxygen sp hybridization. (The oxygen sp hybridization in Si_2O is suppressed by symmetry.) Contrary to the assumption made by Urch[11] and by Reilly,[12] we find that there is a very little oxygen sp hybridization. We also find that d hybridization, although present, is not a very important contribution, contrary to the conclusions of Collins *et al.*[14] An analysis of the SiO wave function also demonstrates that direct crossover transitions in a literal sense make only a very small contribution to the emission lines. The eigenstates are mixtures of atomic components, and the dominant contribution to a transition between valence and core levels is a vertical transition between atomic components on the same atom. We find that the silicon atomic components are strongly modified from their shape in the separated atoms, and that this has an order-of-magnitude effect on the calculated oscillator strengths.

Calculations for collinear Si-O-Si are presented in Sec. IV. The agreement between the calculated and observed positions of the principal peak is good, but the calculated separation between the principal peak and satellite is too large. However, in Sec. V it is shown that bending of the Si-O-Si bond will reduce the calculated separation. Oxygen sp hybridization, and also the $2s(O) \rightarrow 1s(O)$ transition, are completely forbidden by symmetry. The atomic orbital modifications are essentially the same as those found for SiO.

The refinements which will be needed in order to reach the level of accurate predictive calculations are discussed in Sec. V. These include bending of the Si-O-Si bond, adding oxygen neighbors by using an Si_2O_7 fragment, and introducing correlation effects. Beyond these refinements for obtaining an accurate picture of the line structure of the oxygen $K\alpha$ spectrum, there are a host of interesting problems involved in interpreting the broadening of the lines into bands by means of calculations of the influence of more distant neighbors and the motion of the nuclei.

II. $K\alpha$ LINE FOR ATOMIC OXYGEN IN THE HARTREE-FOCK APPROXIMATION

Starting from the $1s^2 2s^2 2p^4$ ground configuration of oxygen, the absorption process excites the atom to a $1s\,2s^2 2p^4$ configuration, which then decays to a $1s^2 2s^2 2p^3$ configuration by emission of an x ray. The allowed transitions are shown in Table I.

The emission-line energies in the Hartree-Fock frozen-orbital approximation are

$$\Delta E = \epsilon_{2p} - \epsilon_{1s} + 2K'_{101}\,G^1(2p, 1s) + [\tfrac{1}{30} - 2K_{112} + 4K'_{112} - \tfrac{9}{4}K''_{112}]\,F^2(2p, 2p)\,, \quad (1)$$

where ϵ_{nl} are the orbital energies in the parent $(1s^2 2s^2 2p^4)$ configuration and $K_{\lambda\mu\nu}$, $K'_{\lambda\mu\nu}$, and $K''_{\lambda\mu\nu}$ are vector coupling coefficients for the parent, excited, and final configurations, respectively.[26] The orbital energies are $\epsilon_{1s} = -562.39$ eV and $\epsilon_{2p} = -17.19$ eV,[27] and the Slater integrals for oxygen in the ^3P state are $G^1(2p, 1s) = 2.873$ eV and $F^2(2p, 2p) = 9.145$ eV. The energy differences for the allowed transitions in the frozen-orbital (FO) approximation are given in the second column of Table II. The orbitals from a ^3P parent state were used for all FO calculations.[28]

The FO approximation neglects the contraction of the occupied orbitals due to the presence of a $1s$ hole in the excited state and a $2p$ hole in the final state. A relaxed-orbital (RO) approximation which takes the hole polarization into account may be ob-

TABLE I. Excitation and decay scheme for atomic oxygen.

Configurations	Parent state $1s^2\,2s^2\,2p^4$	→	Excited state $1s\,2s^2\,2p^4$	→	Final state $1s^2\,2s^2\,2p^3$
Terms	^3P	→	^4P	→	^4S
			^2P	→	^2D, ^2P
	^1D	→	^2D	→	^2D, ^2P
	^1S	→	^2S	→	^2P

tained by using separate SCF calculations for the excited and final hole states and taking the energy difference. The results for RO calculations are shown for comparison in the third column of Table II.[27]

RO calculations for the $K\alpha$ emission-line energies of Na^{++}, Ne^{+}, and F^{-} give the values 1041.0, 848.8, and 677.2 eV, respectively, which may be compared with the corresponding experimental values 1041.1, 848.8, and 676.6 eV.[29] Extrapolating the differences for $Z=11$, 10, 9 and down to $Z=8$, one might infer that RO calculations of the oxygen $K\alpha$ emission lines should give values which are of the order of 1 eV above the experimental values. But we also note that a similar extrapolation on the difference between the FO and RO calculations leads to a predicted difference of 22 eV for oxygen, whereas the actual difference (Table II) is closer to 15 eV. With due allowance for these uncertainties, one is led to expect that the true values for the $K\alpha$ emission lines should lie somewhere between 15 and 25 eV below the values calculated in the FO approximation. We expect the error in RO calculations to be quite small, of the order of 1 eV, but more theoretical and experimental data on a variety of systems are needed before a probable bound as small as this can be assigned with confidence.

Hole polarization has a relatively small (but non-negligible) effect on the separation between emission lines with a common excited state. (Compare the difference between the $^2P\rightarrow{}^2D$ and $^2P\rightarrow{}^2P$ or $^2D\rightarrow{}^2D$ and $^2D\rightarrow{}^2P$ emission-line energies for FO and RO calculations.) It has a much larger effect on the separation between emission lines for different excited states. (Compare the $^4P\rightarrow{}^4S$ and $^2P\rightarrow{}^2D$ lines.) This should not be unexpected, for we know that the error in the calculated term splittings for light atoms can be as large as 50%, and can vary appreciably from one term interval to another.[30] The smaller effect on intervals between satellites with the same excited state is, presumably, due to better cancellation of correlation errors.

The isotropic oscillator strength for an atomic transition in the FO approximation is given by[31]

$$f=\tfrac{2}{3}\Delta E\sum_{M'}|\langle\alpha'L'M'|\textstyle\sum\vec{r}_i|\,\alpha LM\rangle|^2$$
$$=\tfrac{2}{3}N_1\Delta E|\langle\alpha'L'M|\textstyle\sum z_i|\,\alpha LM\rangle|^2$$
$$=\tfrac{2}{3}N_1N_2\Delta E|\langle 1s|z|2p_0\rangle|^2, \qquad (2)$$

where ΔE is the energy separation of the initial and final levels measured in hartrees, α and α' label the initial and final configuration and spin states, L, M and L', M' label the initial and final angular momentum states ($M=L$ or L', whichever is smallest, in the second line), $\langle 1s|z|2p_0\rangle=6.18\times10^{-2}$ B is the dipole matrix element between the $1s$ and $2p_0$ oxygen orbitals in the parent (^3P) state, and N_1 and N_2 are numerical coefficients which are tabulated in Table II. The oscillator strengths for the various transitions in the FO approximation are tabulated in the last column of Table II. Oscillator strengths for the RO approximation were not calculated.

The transition probability for $K\alpha$ emission has been calculated for Ne^{+} in both the FO and RO approximations, and it is found that the RO value is about 40% larger than the FO value.[32] This is primarily due to a change in the value of $\langle 1s|z|2p_0\rangle$ when the contracted orbital is used, so that it should not have as great an effect on the ratio of the line intensities.

The line intensities are actually proportional to the Einstein coefficients for induced transitions, $B=(\pi e^2/m\Delta E)f$. However, the energy level difference ΔE is very nearly the same for the different transitions of interest, so that we may use the oscillator strengths to compare the line intensities. The oscillator strengths have the convenient property that they are dimensionless quantities which

TABLE II. Calculated $K\alpha$ emission spectrum for atomic oxygen.

Transition	Emission Energy ΔE(eV)[a] FO's	RO's	Coefficients[b] N_1	N_2	Oscillator strength for FO's f
$^4P\rightarrow{}^4S$	547.0	531.5	1	$\frac{4}{9}$	0.023
$^2P\rightarrow{}^2D$	546.6	532.4	$\frac{10}{3}$	$\frac{3}{4}$	0.128
$^2P\rightarrow{}^2P$	544.4	529.9	2	$\frac{3}{4}$	0.076
$^2D\rightarrow{}^2D$	546.9	532.1	$\frac{3}{2}$	1	0.077
$^2D\rightarrow{}^2P$	544.7	529.7	2	$\frac{1}{4}$	0.026
$^2S\rightarrow{}^2P$	547.9	532.0	3	$\frac{2}{3}$	0.103

[a]Reference 27.
[b]See Eq. (2).
[c]The $1s^2\,2s^2\,2p^4\,{}^3P$ parent state was used.

obey the Kuhn-Thomas sum rule, $\sum_m f_{nm} = 1$.

If we assume that ^1D and ^1S terms are not excited, so that the only contribution is from the ^3P decay sequence, and introduce the 20-eV correction discussed earlier, then the atomic FO calculations lead to the following predicted oxygen $K\alpha$ spectrum: a dominant peak (coming from the unresolved $^4P \rightarrow {}^4S$ and $^2P \rightarrow {}^2D$ transitions) and a satellite above 2 eV below (from the $^2P \rightarrow {}^2P$ transition), with an intensity ratio of approximately 2:1. The RO calculations suggest a similar spectrum, with a more pronounced broadening of the dominant peak (or, for high resolution, a shoulder on the low-energy side).

It is interesting to compare the *ab initio* atomic SCF calculations, summarized at the bottom of Fig. 4, with the semiempirical molecular calculations, summarized at the bottom of Fig. 1. The former are in at least as good agreement with experiment as the latter. If one were to rely primarily on agreement between the calculated and observed positions of the emission peaks as a test of the validity of a model, one would have to take the atomic model as seriously as the molecular models on the basis of this comparison. However the atomic model cannot be correct because the Si-O overlap is so great that bonding effects must be important; hence, we infer that a much closer agreement between theory and experiment is needed before we can draw conclusions regarding the electronic structure from observations of the emission spectra.

III. OXYGEN $K\alpha$ LINES FOR SiO IN THE HARTREE-FOCK FO APPROXIMATION

The ground state of neutral SiO is $1\sigma^2 2\sigma^2 3\sigma^2 1\pi^4 4\sigma^2 5\sigma^2 6\sigma^2 2\pi^4 7\sigma^2\,{}^1\Sigma$. The MO energies and gross atomic populations are given in Table III for an internuclear separation of $R = 3.104$ B (1.643 Å).[33] The atomic orbital energies of the free atoms are also tabulated for comparison. The orbitals and orbital energies were obtained from the calculations of McLean and Yoshimine.[34] The inner orbitals and levels are primarily atomic in character, with increasing delocalization as one moves out toward the valence levels. The initial state for all $K\alpha$ emission lines is $2\sigma^2\,{}^2\Sigma$, i.e., a $^2\Sigma$ state formed by removing an electron from the 2σ orbital of the parent state. The $5\sigma^2\,{}^2\Sigma$ level is predominantly $2s$(O), i.e., the dominant atomic component of the 5σ MO is a modified oxygen $2s$ atomic orbital, but there is a non-negligible delocalization with consequences which will be discussed in more detail later. The strongly delocalized $6\sigma^2\,{}^2\Sigma$, $2\pi^2\,{}^2\Pi$ and $7\sigma^2\,{}^2\Sigma$ levels are donor levels for the oxygen $K\alpha$ emission spectrum.

The emission energies in the Hartree-Fock FO approximation, given by

$$\Delta E = \epsilon_{i\lambda} - \epsilon_{i_0\lambda_0}\,, \tag{3}$$

are listed in Table IV for $i_0\lambda_0 = 2\sigma$ and $i\lambda = 5\sigma$, 6σ, 2π, and 7σ. Oscillator strengths, calculated from the expression

$$f = \tfrac{2}{3} N \Delta E \left| \langle \Psi | \sum \vec{r}_i | \Psi' \rangle \right|^2 = \tfrac{2}{3} N \Delta E \left| \langle i\lambda | \vec{r} | i_0\lambda_0 \rangle \right|^2 \tag{4}$$

for the same levels, are also listed in Table IV. N is the orbital degeneracy of the final state: $N = 1$ for Σ states and $N = 2$ for Π states. All quantities must be expressed in atomic units [1 hartree(H) = 27.212 eV, 1 bohr(B) = 0.52918 Å] when Eq. (4) is used.

The results in Table IV are summarized graphically and compared with the experimental oxygen

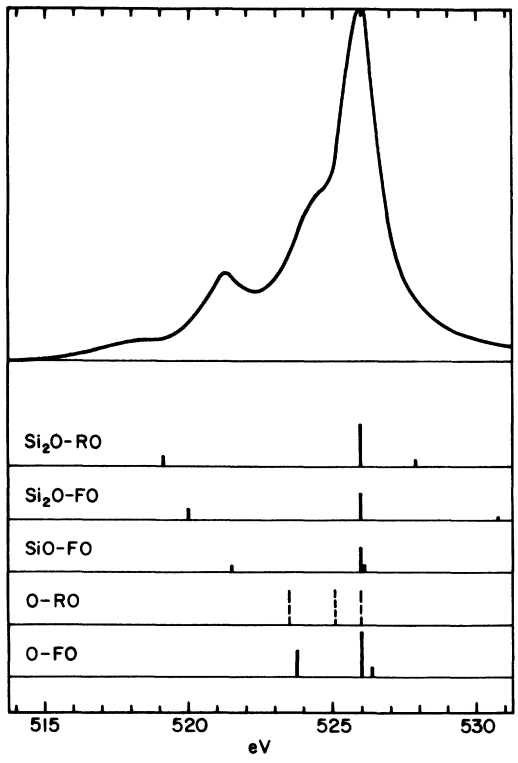

FIG. 4. Comparison of the oxygen $K\alpha$ emission lines calculated for different models with the emission spectrum observed by Klein and Chun (Ref. 2). FO = frozen orbitals, RO = relaxed orbitals. The dominant calculated line has been aligned with the dominant experimental peak at 526 eV. The difference, $\Delta E_{\text{calc}} - \Delta E_{\text{expt}}$, between the calculated and observed positions of the dominant peak are as follows (the quantity in parentheses is the percent error): Collinear Si_2O, RO's, −0.3 eV (0.06%); collinear Si_2O, FO's, 18.8 eV (3.6%); SiO, FO's, 20.7 eV (3.9%); O, RO's, 6.4 eV (1.2%); O, FO's, 20.6 eV(3.9%). The length of the lines representing the calculated emission spectra are proportional to the calculated oscillator strengths, except for O-RO for which oscillator strengths were not calculated.

TABLE III. SiO orbital energies and atomic populations.[a]

$i\lambda$	$nl(A)$	ϵ_{nl}[b]	$\epsilon_{i\lambda}$[c]	$N_{Al}^{i\lambda}$[d]
1σ	$1s$(Si)	−68.812	−68.853	2.00
2σ	$1s$(O)	−20.668	−20.532	2.00
3σ	$2s$(Si)	−6.157	−6.193	2.00
1π	$2p$(Si)	−4.256	−4.295	4.00
4σ	$2p$(Si)	−4.256	−4.292	2.00
5σ	$2s$(O)	−1.244	−1.220	1.77
	$3s$(Si)	−0.540		0.10
	$3p$(Si)	−0.297		0.07
	$2p$(O)	−0.632		0.04
	$3d$(Si)	···		0.02
6σ	$3s$(Si)	−0.540	−0.602	0.92
	$2p$(O)	−0.632		0.91
	$2s$(O)	−1.244		0.13
	$3p$(Si)	−0.297		0.03
	$3d$(O)	···		0.01
2π	$2p$(O)	−0.632	−0.443	3.22
	$3p$(Si)	−0.297		0.59
	$3d$(Si)	···		0.15
	$4f$(Si)	···		0.03
	$3d$(O)	···		0.02
7σ	$3s$(Si)	−0.540	−0.436	0.76
	$2p$(O)	−0.632		0.68
	$3p$(Si)	−0.297		0.54
	$3d$(Si)	···		0.01

[a]Energies in hartrees, 1H = 27.212 eV.

[b]Atomic orbital energies for unmodified orbitals in free atoms. Values are from Ref. 23.

[c]Molecular orbital energies for an internuclear distance of $R = 3.104$ B (1.643 Å). Values are from Ref. 34.

[d]Gross atomic populations. (See Appendix) The total gross atomic populations for Si and O correspond to $Si^{+0.78}O^{-0.78}$.

$K\alpha$ x-ray emission spectrum for silica in Fig. 2. The agreement is rather good, which is unfortunate because the model is not valid for silica. An SiO fragment provides for only a single Si-O bond to each oxygen atom, whereas in silica each oxygen atom is bonded to two silicon atoms.

The SCF-MO's for SiO can, nevertheless, be used to interpret some features of the soft-x-ray emission spectra of silica. On the basis of experience with calculations on a variety of diatomic molecules, we are confident that an SCF calculation provides a reasonably accurate picture of the electronic structure of diatomic SiO, even though some quantitative aspects are not well represented.[35] If the difference between the environment of an oxygen atom in SiO and the environment of an oxygen atom in silica is taken into account, we can use the MO's of SiO in order to obtain some insight into the electronic structure of silica.

A matter of particular interest is the nature of crossover transitions in which an electron in an orbital energy level identified with an atomic orbital of one atomic species drops down into an unoccupied orbital energy level identified with an atomic orbital of another atomic species. The silicon $K\beta$ spectrum of silica provides a classic example of a crossover transition.[36] It contains an emission peak which is clearly identified with an electron from a $2s$(O) level (the 5σ level of SiO) dropping down into a half-occupied $1s$(Si) level (the 1σ level of SiO). The small overlap between a $1s$(Si) and a $2s$(O) orbital raises questions regarding the literal interpretation of this peak as a true crossover transition. One can investigate these questions by using an expansion of the SCF-MO's into their atomic components.

The $2s$(O) emission peak occurs in both the oxygen $K\alpha$ and silicon $K\beta$ spectra of SiO. (Refer to the calculated oscillator strengths for the $2\sigma^2\Sigma \rightarrow 5\sigma^2\Sigma$ hole transition in Table IV and the $1\sigma^2\Sigma \rightarrow 5\sigma^2\Sigma$ hole transition in Table V.) The change in environment in going from SiO to silica suppresses the peak in the oxygen $K\alpha$ spectrum and enhances it in the silicon $K\beta$ spectrum. The 2σ(SiO) and 5σ(SiO) levels both become gerade levels in Si_2O, so that dipole transitions are forbidden. They remain almost forbidden in Si_2O_7 and silica. The 1σ(SiO) and 5σ(SiO) levels go into a_1 and t_2 levels of SiO_4, respectively, between which dipole transitions are allowed. If one constructs an approximate $t_2(SiO_4)$ orbital by taking appropriate linear combinations of 5σ(SiO) orbitals, one finds that the coefficient of the $3p$(Si) atomic component is enhanced by a factor of $2/[3(1-S)]^{1/2}$, where S is the overlap between two normalized 5σ(SiO) orbitals which share a common silicon atom. This factor provides an enhancement of the order of 2 in the oscillator strength. Leaving these qualitative and well-understood differences between SiO and silica aside for the moment, let us analyze the nature of the $5\sigma \rightarrow 1\sigma$ crossover transition in SiO in a little more detail.

The expansion

$$\Psi_{i\lambda}(\vec{r}) = \sum_{Al} B_{i\lambda,Al}\, \varphi_{nl(A)}^{i\lambda}(\vec{r}) \tag{5}$$

TABLE IV. Energies and oscillator strengths for the oxygen $K\alpha$ x-ray emission spectrum of SiO in the Hartree-Fock FO approximation.

Transition[a]	ΔE (eV)	f
$2\sigma\,^2\Sigma \rightarrow 5\sigma\,^2\Sigma$	525.5	0.0007
$2\sigma\,^2\Sigma \rightarrow 6\sigma\,^2\Sigma$	542.3	0.019
$2\sigma\,^2\Sigma \rightarrow 2\pi\,^2\Pi$	546.7	0.070
$2\sigma\,^2\Sigma \rightarrow 7\sigma\,^2\Sigma$	546.8	0.018

[a]Levels are designated by $i\lambda\,^{2s+1}\Lambda$, where $i\lambda$ is the hole in the parent configuration and $^{2s+1}\Lambda$ is the term label.

TABLE V. Energies and oscillator strengths for the silicon $K\alpha$ and $K\beta$ x-ray emission spectra of SiO in the Hartree-Fock FO approximation.

Transition	ΔE (eV)	f
$1\sigma\,^2\Sigma \rightarrow 1\pi\,^2\Pi$ ($K\alpha$)	1756.7	0.158
$1\sigma\,^2\Sigma \rightarrow 4\sigma\,^2\Sigma$ ($K\alpha$)	1756.8	0.079
$1\sigma\,^2\Sigma \rightarrow 5\sigma\,^2\Sigma$ ($K\beta$)	1840.4	0.00030
$1\sigma\,^2\Sigma \rightarrow 6\sigma\,^2\Sigma$ ($K\beta$)	1857.2	0.00038
$1\sigma\,^2\Sigma \rightarrow 2\pi\,^2\Pi$ ($K\beta$)	1861.6	0.00101
$1\sigma\,^2\Sigma \rightarrow 7\sigma\,^2\Sigma$ ($K\beta$)	1861.8	0.00170

of a molecular orbital into its atomic components may be used to analyze dipole matrix elements between molecular levels into components which correspond to hybridization, delocalization, and crossover. (The algorithm for this expansion is described in the Appendix.) The decomposition is

$$\langle i\lambda|\vec{r}|i'\lambda'\rangle = \sum_{AA'll'} B^{*}_{i\lambda,Al} \times \langle nl^{i\lambda}(A)|\vec{r}|n'l'^{i'\lambda'}(A')\rangle B_{i'\lambda',A'l'}. \quad (6)$$

The individual terms in Eq. (6) are not uniquely defined because the atomic components are not orthogonal, so that the individual atomic dipole matrix elements depend on the choice of the origin. In analyzing transitions in which one level is almost purely atomic character, as occurs here, the most reasonable choice is to place the coordinates at the origin of that atom. We shall adopt this prescription.

The 1σ(SiO) and 2σ(SiO) levels are almost purely atomic in character, so that Eq. (5) reduced to a single term:

$$\Psi_{1\sigma(SiO)} \approx \varphi_{1s(Si)}\,, \qquad \Psi_{2\sigma(SiO)} \approx \varphi_{1s(O)}\,. \quad (7)$$

The expansion of the 5σ(SiO) orbital is

$$\Psi_{5\sigma(SiO)} = 0.9088\ \varphi^{5\sigma}_{2s(O)} - 0.1061\ \varphi^{5\sigma}_{2p(O)} + 0.0192\ \varphi^{5\sigma}_{3d(O)} - 0.0044\ \varphi^{5\sigma}_{4f(O)} + 0.1325\ \varphi^{5\sigma}_{3s(Si)} + 0.0917\ \varphi^{5\sigma}_{3p(Si)} + 0.0334\ \varphi^{5\sigma}_{3d(Si)} + 0.0058\ \varphi^{5\sigma}_{4f(Si)}\,. \quad (8)$$

The dipole matrix element decomposition for the $5\sigma \rightarrow 1\sigma$ and $5\sigma \rightarrow 2\sigma$ transitions, obtained by substituting Eqs. (7) and (8) into Eq. (6), are summarized in Table VI. The decomposition is illustrated schematically in Fig. 5.

We note that, for both transitions, a single vertical component provides the dominant contribution. In the $5\sigma \rightarrow 1\sigma$ transition, the $3p$(Si) $\rightarrow 1s$(Si) component contributes 106% of the total dipole matrix element in spite of the fact that the gross atomic population of the $3p$(Si) component is only 4% of the total. The $2s$(O) $\rightarrow 1s$(Si) crossover component contributes only -5% of the total even though the $2s$(O) atomic component comprises 88% of the population of the 5σ(SiO) level. A similar situation occurs for the $5\sigma \rightarrow 2\sigma$ transition, although here the crossover contributions amount to 10% of the total even though the ratio of the gross atomic population of orbitals contributing to crossover and direct transitions has dropped from 23 to 5. The increase in the crossover contribution is obviously due to the more diffuse character of the silicon valence orbitals.

Literally speaking, both the $5\sigma \rightarrow 1\sigma$ and $5\sigma \rightarrow 2\sigma$ transitions are primarily vertical. The oscillator strength of the $5\sigma \rightarrow 1\sigma$ transition is almost completely determined by delocalization; i.e., an admixture of a $3p$(Si) component into a nominally $2s$(O) level, and the oscillator strength of the $5\sigma \rightarrow 2\sigma$ transition is primarily determined by hybridization; i.e., an admixture of a $2p$(O) component. In effect, an electron in a 5σ level resonates (in

TABLE VI. Atomic component analysis of the $\langle 5\sigma(SiO)|z|1s^{1\sigma}(Si)\rangle$ and $\langle 5\sigma(SiO)|z|1s^{2\sigma}(O)\rangle$ dipole matrix elements for $R = 3.104$ B.[a]

$nl(A)$	$B_{5\sigma,Al}$	$\langle nl^{5\sigma}(A)\|z_{Si}\|1s^{1\sigma}(Si)\rangle$	$B_{5\sigma,Al}\langle\|z_{Si}\|\rangle$	$\langle nl^{5\sigma}(A)\|z_{O}\|1s^{2\sigma}(O)\rangle$	$B_{5\sigma,Al}\langle\|z_{O}\|\rangle$
$2s$(O)	0.90879	0.00013	0.00012	0	0
$2p$(O)	−0.10613	−0.00031	0.00003	0.05804	−0.00616
$3d$(O)	0.01915	0.00055	0.00001	0	0
$4f$(O)	−0.00444	−0.00057	0.00000_3	0	0
$3s$(Si)	0.13248	0	0	−0.00216	−0.00029
$3p$(Si)	0.09173	−0.02925	−0.00268	−0.00371	−0.00034
$3d$(Si)	0.03342	0	0	−0.00351	−0.00012
$4f$(Si)	0.00578	0	0	−0.00398	−0.00002
		$\langle 5\sigma(SiO)\|z_{Si}\|1s^{1\sigma}(Si)\rangle = -0.00252$[b]		$\langle 5\sigma(SiO)\|z_{O}\|1s^{2\sigma}(O)\rangle = -0.00693$[c]	

[a] The analysis is based on the expansion $\langle 5\sigma(SiO)| = \Sigma_{Al} B_{5\sigma,Al}\langle nl^{5\sigma}(A)|$. See text. Units for dipole matrix elements are bohrs.

[b] $\langle 5\sigma(SiO)|z|1\sigma(SiO)\rangle = -0.00256$ B.

[c] $\langle 5\sigma(SiO)|z|2\sigma(SiO)\rangle = -0.00722$ B.

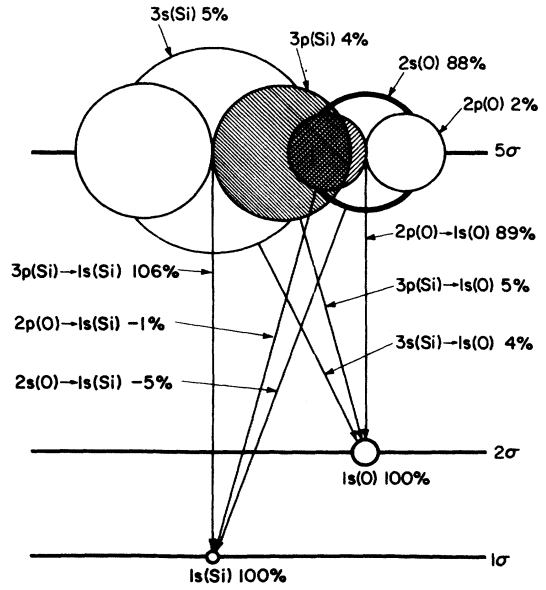

FIG. 5. Schematic representation of the decomposition of the 5σ(SiO) $\rightarrow 2\sigma$(SiO) and 5σ(SiO) $\rightarrow 1\sigma$(SiO) transitions into atomic components. The numbers opposite the atomic component labels [3s(Si) 5%, 3p(Si) 4%, etc.] give the relative gross atomic population, $100 \times (N_{Ai}^{i\lambda}/N_{i\lambda})$, for a given component and level. [The small 3d(Si) and 4f(Si) components of the 5σ(SiO) level have been omitted.] The number opposite the atomic transition labels [3p(Si) → 1s(Si) 106%, etc.] give the relative contribution of the atomic components of the dipole matrix element to the total dipole matrix element: $100 \times B_{5\sigma,Ai}\langle nl(A) \mid z \mid n'l'(A')\rangle / \langle 5\sigma \mid z \mid n'l'(A')\rangle$; $n'l'(A') = 1s$(Si) or $1s$(O).

the sense of Pauling) between modified 2s(O), 2p(O), 3p(Si), and 3s(Si) atomic orbitals, and makes a transition to the 1σ or 2σ level only by a vertical jump from a 3p(Si) to a 1s(Si) orbital or a 2p(O) to a 1s(O) orbital, respectively. The description "delocalization transition" might be more appropriate than "crossover transition" for the $5\sigma \rightarrow 1\sigma$ transition, although the latter designation is still appropriate from the viewpoint of the over-all process.

It is perhaps worth noting that the use of the dipole matrix elements $\langle i\lambda \mid \vec{r} \mid i'\lambda'\rangle$ for calculating molecular transition probabilities in the soft-x-ray region would not be justified if crossover contributions were important. The wavelength of soft x rays is not sufficiently large compared to the interatomic distances to permit one to neglect the exponential term in the matrix elements $\langle i\lambda \mid e^{i\vec{k}\cdot\vec{r}}\vec{p} \mid i'\lambda'\rangle$ from which the formula expressing transition probabilities in terms of dipole matrix elements is obtained. We have, for x rays from the oxygen $K\alpha$ emission spectrum, $\kappa R_{\mathrm{Si-O}} = 0.5$ and $\kappa\langle r\rangle_{1s(O)} = 0.03$, where $\kappa = 2\pi/\lambda = 0.15$ B^{-1} is the wave vector for the x ray, $R_{\mathrm{Si-O}} = 3.1$ B is the nearest-neighbor distance, and $\langle r\rangle_{1s(O)} = 0.20$ B is the mean radius of an oxygen 1s orbital.

There is another interesting bit of information which one may extract from the SCF-MO's for SiO. Referring to Table IV, we note that the $5\sigma \rightarrow 2\sigma$ transition (i.e., the $2\sigma \rightarrow 5\sigma$ hole transition) has an oscillator strength which is only 1% of the oscillator strength of the dominant transition (the $2\pi \rightarrow 2\sigma$ transition). This is consistent with the fact that the coefficient of the 2p(O) component in Eq. (8), which provides the dominant contribution to the oscillator strength, is approximately 0.1. But we also note that the oscillator strength of the $5\sigma \rightarrow 1\sigma$ transition (Table V) is more than 10% of the combined oscillator strengths of the two dominant transitions ($7\sigma \rightarrow 1\sigma$ and $2\pi \rightarrow 1\sigma$). The 3p(Si) populations in the 7σ and 2π levels are less than the 2p(O) populations, so that one would expect some increase in the *relative* intensity of the 5σ line in the silicon $K\beta$ spectrum as compared to the oxygen $K\alpha$ spectrum. But the coefficients of the 2p(O) and 3p(Si) components in the 5σ level [Eq. (8)] are approximately equal, and the ratio of the 2p(O) and 3p(Si) populations in the valence levels is only about 3, so that we must look further in order to explain the order-of-magnitude difference in the relative intensities.

The explanation lies in the modification of the atomic orbitals which occurs when the atoms are brought together to form a molecule. These modifications are relatively small for oxygen orbitals, as may be seen in Fig. 6 where the modified $2p^{7\sigma}$(O), $2p^{2\pi}$(O), $2p^{6\sigma}$(O), and $2p^{5\sigma}$(O) atomic orbitals are compared with the unmodified 2p(O) orbital of an isolated oxygen atom. Within the region of overlap with a 1s(O) orbital the differences are all small, so that the orbital modifications will not have a significant effect on the dipole matrix elements. The situation is quite different for silicon orbitals, as may be seen from Fig. 7. Not only are the differences between the modified and unmodified orbitals much more pronounced, but the pronounced contraction of the orbital tails in-

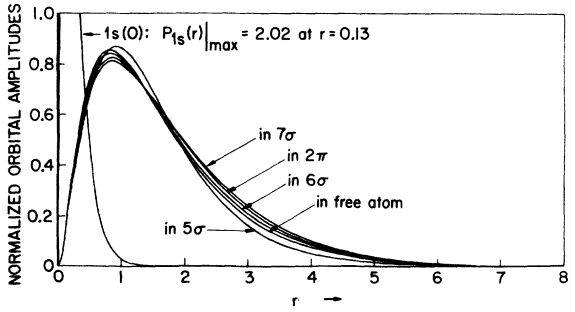

FIG. 6. Modified 2p(O) atomic orbitals in SiO.

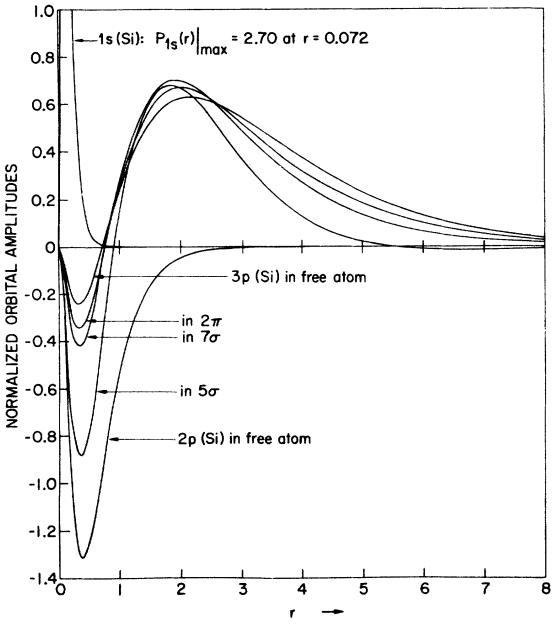

FIG. 7. Modified $3p$(Si) atomic orbitals in SiO.

creases the amplitude within the K and L shells by a factor which can be greater than 3.

The quantitative effect of these modifications on the dipole matrix elements may be seen more precisely in Table VII where the dipole matrix elements of the modified $2p$(O) and $3p$(Si) orbitals are compared with each other and with the dipole matrix elements for the corresponding unmodified orbitals. The oxygen matrix elements are all comparable. The $3p^{5\sigma}$(Si) matrix element is larger than the $3p$(Si) matrix element by a factor of 3.6, and larger than the $3p^{7\sigma}$(Si) and $3p^{2\pi}$(Si) matrix elements by factors of 2.1 and 2.5, respectively. The valence orbital contraction which occurs when a silicon atom is placed in an SiO molecular environment can, therefore, enhance the intensity of the 5σ satellite in the silicon $K\beta$ spectrum of SiO by a factor of approximately 5.

This example of orbital modification in molecules serves to emphasize the fact that LCAO calculations are not reliable for calculating x-ray emission intensities. Orbital relaxation and correlation effects can introduce errors which approach a factor of 2 in some cases (see Secs. IV and V), but orbital modifications can introduce order-of-magnitude errors which make a comparison between observed and calculated results rather meaningless.

Returning to Table III we note that the d hybridization of the orbitals is rather small. The greatest d hybridization occurs in the 2π(SiO) orbital where the $3d$(Si) population is 4% of the total. This is in contrast to the results of the calculations of Collins *et al.*[14] who obtain rather large $3d$ populations for SiO_4. While one might argue that it is possible for the additional oxygen neighbors to cause a marked increase in the silicon d population, we are inclined to believe that their result is a property of their basis sets and not of the system. It has been our experience that when basis functions of higher symmetry are added to a minimal basis set without first augmenting with basis functions of lower symmetry, these added basis functions will attempt to remedy the deficiencies of the basis set of lower symmetry. We expect that if SiO_4 calculations were done with nominal or accurate s and p basis sets for silicon, the d hybridization would be much closer to that which McLean and Yoshimine obtain for SiO than that which Collins *et al.* obtain for SiO_4.

IV. OXYGEN $K\alpha$ LINES FOR COLLINEAR Si-O-Si IN THE HARTREE-FOCK APPROXIMATION

The configuration of neutral collinear Si_2O is

$$1\sigma_g^2 1\sigma_u^2 2\sigma_g^2 3\sigma_g^2 2\sigma_u^2 4\sigma_g^2 3\sigma_u^2 1\pi_u^4 1\pi_g^4 5\sigma_g^2 4\sigma_u^2 2\pi_u^4 6\sigma_g^2 5\sigma_u^2 2\pi_g^2. \quad (9)$$

This is an open-shell configuration with three terms: $^3\Sigma_g^-$, $^1\Delta_g$, and $^1\Sigma_g^+$. Self-consistent-field energies, orbitals and orbital energies, atomic populations and dipole matrix elements were calculated for these terms using the ALCHEMY computer program.[37] The optimized basis set determined by McLean and Yoshimine for SiO was used.[34] In view of the similarity of SiO and Si_2O, it was assumed that the accuracy of the calculations for the two systems would be comparable without further optimization of the basis function exponents.

TABLE VII. Comparison of dipole matrix elements (in bohrs) of some modified and unmodified atomic orbitals.

Oxygen $2p$
$\langle 2p^{5\sigma}(O) \mid z \mid 1s(O)\rangle = 0.0579$
$\langle 2p^{6\sigma}(O) \mid z \mid 1s(O)\rangle = 0.0606$
$\langle 2p_x^{2\pi}(O) \mid x \mid 1s(O)\rangle = 0.0591$
$\langle 2p^{7\sigma}(O) \mid z \mid 1s(O)\rangle = 0.0579$
$\langle 2p(O) \mid z \mid 1s(O)\rangle = 0.0618$
Silicon $3p$
$\langle 2p(Si) \mid z \mid 1s(Si)\rangle = 0.0429$
$\langle 3p^{5\sigma}(Si) \mid z \mid 1s(Si)\rangle = -0.0293$
$\langle 3p_x^{2\pi}(Si) \mid x \mid 1s(Si)\rangle = -0.0115$
$\langle 3p^{7\sigma}(Si) \mid z \mid 1s(Si)\rangle = -0.0139$
$\langle 3p(Si) \mid z \mid 1s(Si)\rangle = -0.0081$

TABLE VIII. Excitation and decay scheme for collinear Si-O-Si.

Configuration	Parent state [Eq. (9)]	Excited state $2\sigma_g$ hole	$4\sigma_u$ hole	Final state $2\pi_u$ hole	$5\sigma_u$ hole
Terms	$^3\Sigma_g^-$ →	$^2\Sigma_g^-$ →	$^2\Sigma_u^-$	$^2\Pi_u$	$^2\Sigma_u^-$
		$^4\Sigma_g^-$ →	$^4\Sigma_u^-$	$^4\Pi_u$	$^4\Sigma_u^-$
	$^1\Delta_g$ →	$^2\Delta_g$ →	$^2\Delta_u$	$^2\Pi_u$, $^2\Phi_u$	$^2\Delta_u$
	$^1\Sigma_g^+$ →	$^2\Sigma_g^+$ →	$^2\Sigma_u^+$	$^2\Pi_u$	$^2\Sigma_u^+$

Only those selected results which are relevant for interpreting the oxygen $K\alpha$ x-ray emission spectrum are included in this article. A complete listing of energies, orbital expansion coefficients, and selected molecular properties for all three states has been deposited with the National Auxiliary Publications Service.[38]

The excitation and decay scheme for the states which contribute to the oxygen $K\alpha$ emission spectrum are shown in Table VIII. The orbital energies and gross atomic populations for the different atoms and atomic symmetries are listed in Table IX for all three terms and all 15 occupied orbitals.

The atomic populations and the orbital energies of interest are essentially the same for all three parent terms: the differences between the $2\sigma_g$, $4\sigma_u$, $2\pi_u$ and $5\sigma_u$ orbital energies vary by less than 0.02 eV from one parent term to another. The open shell (the $2\pi_g$ shell) has an oxygen atomic population of only 0.02 for all terms, so that differences in the electronic structure of the three terms should have very little effect on the electronic structure of the oxygen atom. Hence, we may limit our attention to a single branch of the excitation and decay sequence. The branch starting from the nondegenerate $^1\Sigma_g^+$ parent term has been chosen for this purpose.

The coefficients for the expansions of the MO's into modified atomic orbitals (MAO's) [Eq. (A4)] are given in Table X for the $^1\Sigma_g^+$ state. The MAO's are portrayed in Figs. 8–10. The modifications are similar to those found earlier for SiO, except that the $2p^{5\sigma_u}$(O) orbital, which is a minor component of the $5\sigma_u(Si_2O)$ orbital, is appreciably extended. Aside from the $3p^{2\pi_g}$(Si) orbital, which does not contribute to the oxygen $K\alpha$ emission spectrum, the modified 3p(Si) orbitals are strongly contracted, as before.

The atomic populations on the different atoms have been identified with an atomic shell (labeled by the principal quantum number n) as well as by an angular momentum. This identification should not be taken too literally, for the atomic orbitals are modified relative to the orbitals in isolated atoms. The identification is made on the basis of orbital energy considerations, identifying a component with the shell of that symmetry for which the undistorted atomic and molecular orbital energies differ least.

We note that there is some d hybridization, but it is rather small: the largest amount being for the $2\pi_u$ orbital in which there is a 3d(Si) atomic population of 0.1 on *each* silicon atom. (Other typical silicon d hybridizations *per atom* are 0.01 for $5\sigma_g$, 0.003 for $6\sigma_g$, 0.01 for $4\sigma_u$ and $5\sigma_u$, and −0.001 for $2\pi_g$.) This is, again, in contrast to the rather large d hybridization obtained by Collins *et al.*[14] The comments made at the end of Sec. III concerning the d hybridization in SiO are applicable here also.

The energy differences corresponding to the emission lines of interest, obtained from Eq. (3) with $i_0\lambda_0 = 2\sigma_g$ and $i\lambda = 5\sigma_g$, $4\sigma_u$, $2\pi_u$, and $5\sigma_u$, are tabulated in Table XI. The oscillator strengths, computed from the dipole moments using Eq. (4), are also listed. The results for the FO calculations are given in the second and fourth columns. The results for RO calculations are given in the third and fourth columns. A graphical comparison with the other calculations and with the observed oxygen $K\alpha$ emission spectrum of silica is given in Fig. 4.

Although the collinear Si_2O model corresponds more closely to the true structure of silica than the SiO model, the agreement between the observed and calculated satellite interval is slightly worse. The observed separation between the primary and satellite peaks in silica is 5 eV. The calculated separation is 4.4 eV for SiO in the FO approximation, 6 eV for collinear Si_2O in the FO approximation, and 6.9 eV for collinear Si_2O in the RO approximation.

The intensity ratios of the primary lines to the satellite are 4.6:1 for the SiO-FO calculation, 2.4:1 for the Si_2O-FO calculation, and 3.9:1 for the Si_2O-RO calculation. The uncertainty in the

TABLE IX. Collinear Si-O-Si orbital energies and atomic populations.[a]

			$^3\Sigma_g^-$		$^1\Delta_g$		$^1\Sigma_g^+$	
$i\lambda$	$nl(A)$	ϵ_{nl}	$\epsilon_{i\lambda}$	$N_{Al}^{i\lambda}$	$\epsilon_{i\lambda}$	$N_{Al}^{i\lambda}$	$\epsilon_{i\lambda}$	$N_{Al}^{i\lambda}$
$1\sigma_g$	1s(Si)	−68.812	−68.810	2.00	−68.812	2.00	−68.814	2.00
$1\sigma_u$	1s(Si)	−68.812	−68.810	2.00	−68.812	2.00	−68.814	2.00
$2\sigma_g$	1s(O)	−20.668	−20.622	2.00	−20.623	2.00	−20.624	2.00
$3\sigma_g$	2s(Si)	−6.157	−6.154	2.00	−6.156	2.00	−6.158	2.00
$2\sigma_u$	2s(Si)	−6.157	−6.154	2.00	−6.156	2.00	−6.158	2.00
$4\sigma_g$	2p(Si)	−4.256	−4.256	2.00	−4.258	2.00	−4.260	2.00
$3\sigma_u$	2p(Si)	−4.256	−4.256	2.00	−4.258	2.00	−4.260	2.00
$1\pi_u$	2p(Si)	−4.256	−4.255	4.00	−4.257	4.00	−4.259	4.00
$1\pi_g$	2p(Si)	−4.256	−4.255	4.00	−4.257	4.00	−4.258	4.00
$5\sigma_g$	2s(O)	−1.244	−1.392	1.81	−1.393	1.81	−1.394	1.81
	3s(Si)	−0.540		0.09		0.09		0.09
	3p(Si)	−0.297		0.08		0.08		0.08
	3d(Si)	···		0.02		0.02		0.02
$4\sigma_u$	2p(O)	−0.632	−0.821	1.45	−0.822	1.45	−0.823	1.45
	3s(Si)	−0.540		0.40		0.40		0.40
	3p(Si)	−0.297		0.12		0.12		0.12
	3d(Si)	···		0.03		0.03		0.03
$2\pi_u$	2p(O)	−0.632	−0.600	3.34	−0.601	3.33	−0.602	3.33
	3p(Si)	−0.297		0.39		0.39		0.39
	3d(Si)	···		0.20		0.20		0.20
	4f(Si)	···		0.07		0.07		0.07
$6\sigma_g$	3s(Si)	−0.540	−0.469	1.78	−0.470	1.78	−0.471	1.78
	3p(Si)	−0.297		0.20		0.19		0.19
	2s(O)	−1.244		0.02		0.02		0.02
	3d(Si)	···		0.01		0.01		0.01
$5\sigma_u$	3s(Si)	−0.540	−0.424	1.50	−0.425	1.50	−0.426	1.50
	3p(Si)	−0.297		0.38		0.38		0.38
	2p(O)	−0.632		0.11		0.11		0.11
	3d(Si)	···		0.02		0.02		0.02
$2\pi_g$	3p(Si)	−0.297	−0.203	1.98	−0.182	1.98	−0.162	1.98
	3d(O)	···		0.02		0.02		0.02

[a]Atomic orbital energies ϵ_{nl} are from Ref. 23. Molecular orbital energies $\epsilon_{i\lambda}$ have been calculated for each term for an internuclear distance of $R=3.02$ B (1.6 Å). All energies are in hartrees, 1 H = 27.212 eV. $N_{Al}^{i\lambda}$ are the gross atomic populations (see the Appendix). The silicon populations are the sum of the gross atomic populations for both silicon atoms. The total gross atomic populations for Si and O correspond to a $Si_2^{+0.37}$ $O^{-0.74}$ charge state. The total energies for the three states are $E(^3\Sigma_g^-) = -652.7186$ H, $E(^1\Delta_g) = -652.6974$ H, and $E(^1\Sigma_g^+) = -652.6763$ H.

TABLE X. Expansion coefficients $B_{i\lambda,Al}$, for the expansion of molecular orbitals for the valence shell of the $^1\Sigma_g^+$ state of collinear Si_2O in modified atomic orbitals: $\Psi_{i\lambda}(\vec{r}) = \sum_{Al} B_{i\lambda} \varphi_{nl(A)}^{i\lambda}(\vec{r})$.[a]

$i\lambda$ \ $nl(A)$	2s(O)	2p(O)	3d(O)	4f(O)	3s(Si)	3p(Si)	3d(Si)	4f(Si)
$5\sigma_g$	0.91257	···	0.03441	···	0.07928	0.06434	0.02661	0.00588
$4\sigma_u$	···	−0.76098	···	−0.01644	0.23767	0.09739	0.04131	0.00804
$2\pi_u$	···	0.85363	···	0.01137	···	0.14305	0.06923	0.02329
$6\sigma_g$	0.32341	···	0.00018	···	−0.70321	0.18690	0.02133	0.00053
$5\sigma_u$	···	−0.47236	···	−0.00979	−0.73036	0.22435	0.03403	0.00268
$2\pi_g$	···	···	−0.02794	···	···	0.75703	0.00981	0.00360

[a]Coefficients are given only for the left silicon atom, Si(1). The relation between the coefficients for A = Si(1) and A' = Si(2) is $B_{i\lambda,Al} = \pm(-1)^l B_{i\lambda,A'l}$, where the +(−) sign applies to gerade (ungerade) states, respectively. Blank entries are coefficients which vanish identically for reasons of symmetry.

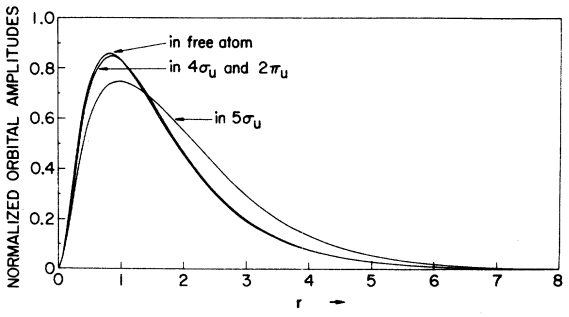

FIG. 8. Modified $2p$(O) atomic orbitals in collinear Si_2O.

magnitudes of the integrated intensities for the primary and satellite bands in silica prevents a meaningful quantitative comparison of calculated and observed intensities. All that one can really say is that the experimental ratio probably lies between 4:1 and 8:1, which is in reasonable (but inconclusive) agreement with the collinear Si_2O-RO calculation.

The most marked improvement is in the position of the dominant peak. The difference between the SiO and collinear Si_2O models appears to be relatively unimportant for the primary peak position; the improvement is primarily due to orbital relaxation. The error in the FO approximation is about 20 eV, or close to 4% for both the SiO and collinear Si_2O models. It drops to less than 1 eV (less than 0.1%) for the RO approximation. This agreement, together with previous work which provides evidence for the reliability of RO calculations of x-ray emission spectra,[27,29] is the strongest quantitative evidence available in support of the identification of the $2\sigma_g\,^2\Sigma_g^+ \rightarrow 2\pi_u\,^2\Pi_u$ transition in Si_2O with the primary emission peak.

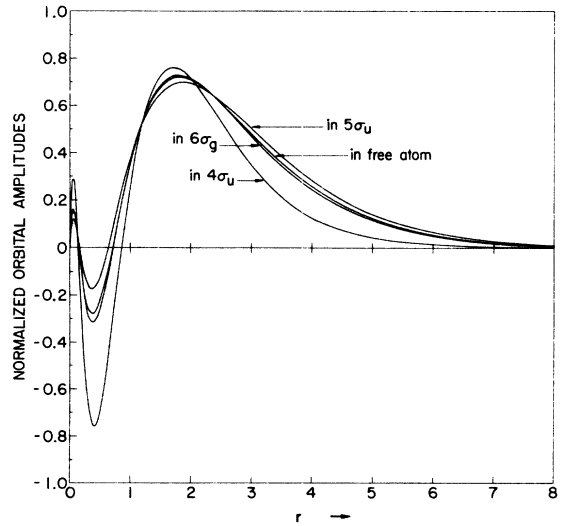

FIG. 9. Modified $3s$(Si) atomic orbitals in collinear Si_2O.

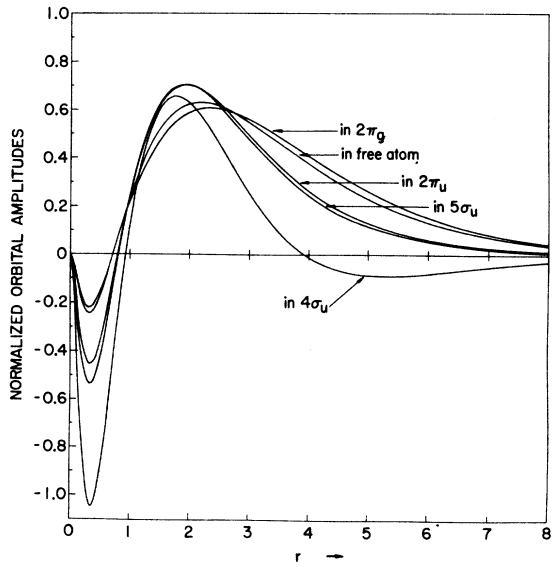

FIG. 10. Modified $3p$(Si) atomic orbitals in collinear Si_2O.

The predicted high-energy satellite at 528 eV (the $2\sigma_g\,^2\Sigma_g^+ \rightarrow 5\sigma_u\,^2\Sigma_u^+$ transition) will be more strongly influenced by the environment than the other transitions, so that a comparison with the observed emission spectrum in silica is not justified. The emission peak corresponding to a $2s$(O) donor level (the $2\sigma_g\,^2\Sigma_g^+ \rightarrow 5\sigma_g\,^2\Sigma_g^+$ transition) does not occur because it is forbidden by symmetry, as noted earlier.

The net charge on the oxygen atom, as measured by the gross atomic population, drops from −0.78 in SiO to −0.74 in Si_2O. The large decrease in the silicon charge, from +0.78 to +0.37, suggests that the silicon charge is rather sensitive to the environment. This is consistent with the fact that the

TABLE XI. Transition energies and oscillator strengths for the oxygen $K\alpha$ x-ray emission spectrum of collinear Si-O-Si.[a]

Transition	ΔE (eV) FO's	ΔE (eV) RO's	f FO's	f RO's
$2\sigma_g\,^2\Sigma_g^+ \rightarrow 5\sigma_u\,^2\Sigma_u^+$	549.6	527.6	0.007	0.015
$2\sigma_g\,^2\Sigma_g^+ \rightarrow 2\pi_u\,^2\Pi_u$	544.8	525.7	0.076	0.122
$2\sigma_g\,^2\Sigma_g^+ \rightarrow 4\sigma_u\,^2\Sigma_u^+$	538.8	518.8	0.032	0.031
$2\sigma_g\,^2\Sigma_g^+ \rightarrow 5\sigma_g\,^2\Sigma_g^+$	523.3	···	0	0

[a]The $^1\Sigma_g^+$ parent state was used.

silicon valence orbitals are quite extended. The more compact oxygen orbitals can be expected to be less sensitive to the environment. Adding another silicon ion introduces Coulomb repulsion between the silicon ions. A decrease in the silicon charge lowers the total energy by decreasing this repulsive energy, as well as maintaining the charge balance.

In going from an Si_2O fragment to an Si_2O_7 fragment, which can be expected to have an ionicity very close to that of bulk silica, the silicon charge will increase in order to maintain the charge balance. We can also expect some change in the oxygen charge. We speculate that this change will be a small decrease in order to reduce the increase in total energy introduced by the Coulomb repulsion between the oxygen ions. A charge configuration of $Si^{+1}O_2^{-0.5}$ would not surprise us. A charge configuration as ionic as $Si^{+2}O_2^{-1}$ would surprise us.

Further refinements are clearly needed in order to converge to reasonable quantitative agreement with the observed interval between the primary and satellite peaks and to explain the shoulder on the low-energy side of the primary peak. These refinements, which are beyond the scope of the *ab initio* calculations undertaken for this study, are discussed in Sec. V.

V. REFINEMENTS

Three refinements are needed to extend the calculations to the point where they can be used for accurate quantitative interpretations and predictions: (a) bending of the Si-O-Si fragment; (b) inclusion of more distant neighbors; and (c) electronic correlation. The effect of bending is of particular interest because it will introduce a qualitatively new feature; viz., splitting of the dominant peak. The effect of bending will be discussed in some detail below. The remaining effects will be considered only very briefly because there is not much that can be said without undertaking detailed calculations which are beyond the scope of this study.

TABLE XII. Occupied Si-O-Si orbitals.

Bent Si_2O	Collinear Si_2O	Major atomic components[a]
$1a_1$	$1\sigma_g$	1s(Si)
$1b_1$	$1\sigma_u$	1s(Si)
$2a_1$	$2\sigma_g$	1s(O)
$3a_1$	$3\sigma_g$	2s(Si)
$2b_2$	$2\sigma_u$	2s(Si)
$4a_1$	$4\sigma_g$	2p(Si)
$3b_2$	$3\sigma_u$	2p(Si)
$5a_1$	$1\pi_u$	2p(Si)
$1b_1$	$1\pi_u$	2p(Si)
$1a_2$	$1\pi_g$	2p(Si)
$4b_2$	$1\pi_g$	2p(Si)
$6a_1$	$5\sigma_g$	2s(O)
$5b_2$	$4\sigma_u$	2p(O), 3s(Si), 3p(Si)
$7a_1$	$2\pi_u$	2p(O), 3p(Si), 3d(Si)
$2b_1$	$2\pi_u$	2p(O), 3p(Si), 3d(Si)
$8a_1$	$6\sigma_g$	3s(Si), 3p(Si)
$6b_2$	$5\sigma_u$	3s(Si), 3p(Si), 2p(O)
$2a_2$	$2\pi_g$	3p(Si)
$7b_2$	$2\pi_g$	3p(Si)

[a]Components with gross atomic populations greater than 0.1 (see Table IX).

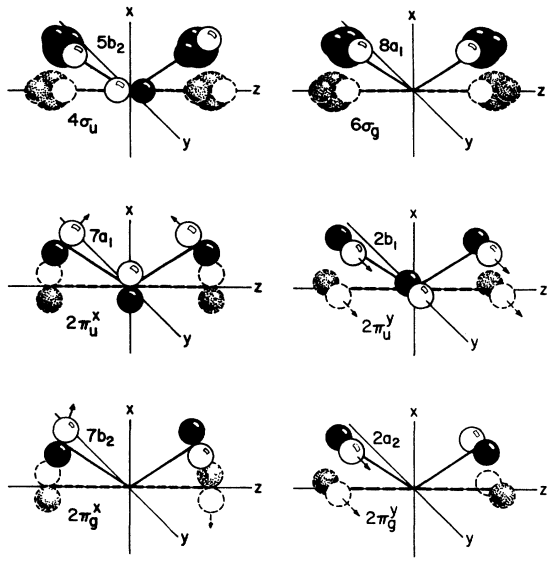

FIG. 11. Symmetry orbitals for collinear and bent Si_2O.

A. Bending Effects

Bending of the Si-O-Si fragment reduces the symmetry from $D_{\infty h}$ to C_{2v}. All degeneracies are lifted. The occupied orbitals are shown in Table XII. If the axes are chosen as shown in Fig. 11, then the a (b) orbitals are those which are even (odd) under 180° rotations about the x axis, and the orbitals with subscripts 1 (2) are those which are even (odd) under reflection in the xy plane. The shaded and unshaded circles in Fig. 11 indicate orbital amplitudes of opposite sign. Only the dominant s and p components are indicated, using an obvious schematic representation. Note that the silicon p orbitals may rotate independently in the a_1 and b_2 symmetry orbitals. The relative amplitudes of the different components for the collinear case may be obtained from Table X.

The correspondence between the parent states of the collinear and bent molecules is as follows:

$$\cdots 2\pi_g^2\ {}^3\Sigma_g^- \rightarrow \cdots 2a_2 7b_2\ {}^3B_1\ ,$$

$$\cdots 2\pi_g^2\,{}^1\Delta_g \rightarrow \begin{cases} [\cdots 2a_2^2\,{}^1A_1] - [\cdots 7b_2^2\,{}^1A_1], \\ \cdots 2a_2 7b_2\ {}^1B_1, \end{cases} \quad (10)$$

$$\cdots 2\Pi_g^2\,{}^1\Sigma_g^+ \rightarrow [\cdots 2a_2^2\,{}^1A_1] + [\cdots 7b_2^2\,{}^1A_1],$$

where $\cdots$ signifies the closed shells, which consist of the shells in all but the last two lines of Table XII. In a single-configuration approximation the $^1A_1$ states would be $\cdots 2a_2^2\,{}^1A_1$ and $7b_2^2\,{}^1A_1$. Mixing of these two configurations is necessary in order to obtain proper correspondence with the terms of the ground configuration of the collinear molecule. The excitation and decay sequence for the term arising from the $^1\Sigma_g^+$ term of the collinear molecule is

$$\begin{aligned} &\text{parent state:} && {}^1A_1 \\ &\text{excited state:} && 2a_1\,{}^2A_1 \\ &\text{final states:} && 5b_2\,{}^2B_2,\quad 2b_1\,{}^2B_1, \\ & && 8a_1\,{}^2A_1,\quad 6b_2\,{}^2B_2, \end{aligned} \quad (11)$$

where the orbital symbol labels the hole in the parent configurations. Decay sequences for the other parent states may be obtained from the orbital correspondence

$$\begin{aligned} &\sigma_g \rightarrow a_1,\quad \sigma_u \rightarrow b_2, \\ &\pi_g^x \rightarrow b_2,\quad \pi_u^x \rightarrow a_1, \\ &\pi_g^y \rightarrow a_2,\quad \pi_u^y \rightarrow b_1, \end{aligned} \quad (12)$$

[where $\pi^{\pm} = (\pi^x \pm i\pi^y)/2^{1/2}$], and the term correspondence,

$$\begin{aligned} &\Sigma_g^+ \rightarrow A_1,\quad \Pi_u \rightarrow A_1 + B_1, \\ &\Sigma_g^- \rightarrow B_1,\quad \Pi_g \rightarrow A_2 + B_2, \\ &\Sigma_u^+ \rightarrow B_2,\quad \Delta_g \rightarrow A_1 + B_1, \\ &\Sigma_u^- \rightarrow B_1,\quad \Delta_u \rightarrow A_2 + B_2. \end{aligned} \quad (13)$$

The following reasoning may be used in order to obtain a qualitative estimate of the effect of bending on the separation of the peaks in the emission spectrum.

Three different bonds are involved in each MO of Si_2O: two Si-O bonds and one Si-Si bond. One might be tempted to assume that the Si-Si bond was weak and made only a small contribution to the orbital energy, but inspection of the overlap integrals for the modified atomic orbitals provides convincing evidence that this is not so. The relevant overlaps are listed in Table XIII. The Si-O overlaps are given for the SiO bond distance of 3.02 B. The Si-Si overlaps are given for the Si-Si bond distance in the collinear fragment (6.04 B), for a fragment bent to an angle of 144° (5.74 B) and a fragment bent to an angle of 90° (4.27 B).

We assume that bending will have a relatively small effect on the energy of the Si-O bond, so that the energy changes will be primarily due to changes in the energy of the Si-Si bond. A reliable quantitative estimate of this contribution cannot be given without undertaking detailed calculations which are beyond the scope of this study. However, a qualitative estimate, i.e., a determination of the direction in which the orbital energy levels move and the order of the final levels, can be obtained by considering an Si_2 fragment and examining the bonding or antibonding characteristics of the MO's for Si_2. If the Si_2 component of an Si_2O molecular orbital is a bonding orbital, then bending the Si_2O fragment will lower that level. Conversely, if the Si_2 component is an antibonding orbital, bending will raise that level.

We may invoke the general rule that, in a homonuclear diatomic molecule, the σ_g and π_u orbitals are bonding orbitals, while the σ_u and π_g orbitals are antibonding. As the Si_2O fragment is bent, the $7a_1$ and $2b_1$ orbital energy levels (which come from the $2\pi_u$ level) will go down and the $5b_2$ and $6b_2$ levels (which come from the $4\sigma_u$ and $5\sigma_u$ levels) will go up. The bonding orbitals are those for which the component overlaps are positive (i.e., the atomic orbitals in Fig. 11 have the same shading in the regions closest to each other), while the antibonding orbitals are those for which the component overlaps are negative (i.e., the atomic orbitals in Fig. 11 have opposite shading in the regions closest to each other). The magnitude of the overlap provides a rough measure of the magnitude of the bonding or antibonding effect. We infer by inspection of the geometry (Fig. 11) that the $7a_1$ level will drop more than the $2b_1$ level, thereby splitting the original $2\pi_u$ level. Similarly, the $7b_2$ level should rise more than the $2a_2$ level.

Using these qualitative considerations as a guide, we infer that bending will change the orbital energy levels in the manner indicated in Fig. 12. We have no reliable way of inferring the magnitude of these changes without further calculations, so that the magnitudes of the displacements shown in Fig. 12 have no significance. The directions of the changes are significant, insofar as one can trust the reasoning outlined above. It is encouraging to note that the changes are in the proper direction to restore at least some of the quantitative agreement which was lost in going from an SiO fragment to a collinear Si_2O fragment.

We looked into the possibility of obtaining a semiquantitative estimate of the changes by doing a simple Hückel-type calculation. If one knew the off-diagonal matrix elements of the Hartree-Fock operator between the atomic components for the collinear molecule, it would not be unreasonable to use the atomic overlaps in the spirit of extended Hückel theory in order to obtain a crude estimate of the Hartree-Fock operator for the bent frag-

TABLE XIII. Overlap integrals between modified and unmodified atomic orbitals in Si_2O.[a]

		$\langle nl^{i\lambda}(A) \mid n'l'^{i\lambda}(A')\rangle_{\sigma,\pi}$			
	$i\lambda$	$R=3.02$	4.27	5.74	6.04 B
$\langle 2p(O) \mid 3s(Si)\rangle_\sigma$	free	0.26433	...	...	...
	$4\sigma_u$	0.25032	...	...	...
	$5\sigma_u$	0.33543	...	...	...
$\langle 2p(O) \mid 3p(Si)\rangle_\sigma$	free	0.19016	...	...	...
	$4\sigma_u$	0.26701	...	...	...
	$2\pi_u$	0.24851	...	...	...
	$5\sigma_u$	0.26538	...	...	...
$\langle 2p(O) \mid 3p(Si)\rangle_\pi$	free	0.23352	...	...	...
	$4\sigma_u$	0.10465	...	...	...
	$2\pi_u$	0.21288	...	...	...
	$5\sigma_u$	0.26229	...	...	...
$\langle 3s(Si) \mid 3s(Si')\rangle_\sigma$	free	...	0.29266	0.12392	0.10187
	$4\sigma_u$	...	0.14800	0.04453	0.03399
	$6\sigma_g$	...	0.30546	0.13192	0.10886
	$5\sigma_u$	...	0.33673	0.15167	0.12621
$\langle 3s(Si) \mid 3p(Si')\rangle_\sigma$	free	...	0.43478	0.25028	0.21796
	$4\sigma_u$	...	0.07122	−0.02213	−0.02836
	$6\sigma_g$	...	0.38362	0.20625	0.17712
	$5\sigma_u$	...	0.33644	0.17098	0.14478
$\langle 3p(Si) \mid 3p(Si')\rangle_\sigma$	free	...	0.31720	0.30203	0.28266
	$4\sigma_u$	...	0.16287	0.00099	−0.01379
	$2\pi_u$	...	0.32558	0.20252	0.17581
	$6\sigma_g$	...	0.32794	0.24141	0.21666
	$5\sigma_u$	...	0.31515	0.18392	0.15749
	$2\pi_g$	...	0.30241	0.32807	0.31269
$\langle 3p(Si) \mid 3p(Si')\rangle_\pi$	free	...	0.29759	0.13813	0.11674
	$4\sigma_u$	...	0.01055	−0.01032	−0.00947
	$2\pi_u$	...	0.17859	0.06383	0.05128
	$6\sigma_g$	...	0.22203	0.08989	0.07405
	$5\sigma_u$	...	0.15996	0.05408	0.04293
	$2\pi_g$	...	0.33527	0.16402	0.13994

[a]The Si-O distance in Si_2O is 3.02 B. The Si-Si distance is 6.04 B in collinear Si_2O, 5.74 B for ∠ Si-O-Si = 1.44°, and 4.27 B for ∠ Si-O-Si = 90°. $\langle \mid \rangle_\sigma$ is the overlap for p orbitals oriented along the line of centers and $\langle \mid \rangle_\pi$ is the overlap for p orbitals oriented perpendicular to the line of centers.

ment. However, circumstances were such that it was not easy to extract the relevant matrix elements from the calculations made with the ALCHEMY computer program, and the reliability of procedures based on Hückel approximations is open to serious question; hence, we decided to settle for the qualitative study of bending outlined above.

B. Larger Fragments

The logical next step for refining the calculations would be to use a larger fragment. An energy level for an Si_2O fragment which was predominantly of oxygen character would become a band of seven lines in an Si_2O_7 fragment. The Si_2O_7 fragment would be a bipyramidal structure obtained by adding an equilateral array of three oxygen atoms at each to form two tetrahedra with a common oxygen vertex and bases rotated by 30° with respect to each other. (See Fig. 2.) The oxygen-oxygen overlap (for unmodified orbitals) is $\langle 2p(O) \mid 2p(O')\rangle_\sigma = 0.0631$ and $\langle 2p(O) \mid 2p(O')\rangle_\pi = 0.0151$ for $R = 5$ B (the distance between neighboring oxygen atoms in silica).

If the charge on the central oxygen atom did not change, then one could argue that the added neighbors would decrease the satellite separation. The added neighbors would raise the potential of the silicon atoms relative to the central oxygen atom, which would raise the $4\sigma_u$ level relative to the $2\pi_u$ level (because the latter has a higher oxygen-to-silicon population ratio). This argument would still be valid if the charge on the central oxygen atom decreased, provided that the oxygen-to-silicon population ratio of the $2\pi_u$ level remained

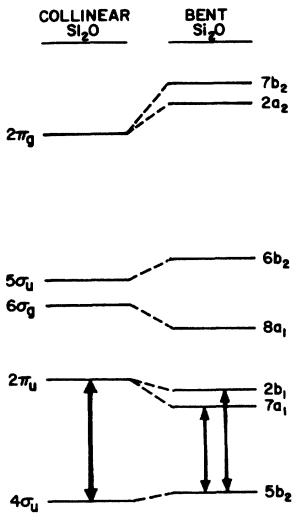

FIG. 12. Orbital energy levels for collinear and bent Si_2O. The diagram for the levels of the bent fragment was obtained from qualitative considerations and is intended only to show the direction of the displacements. (See text.) The double arrows indicate the separation between the principal peak and the low-energy satellite, not a transition.

higher than for the $4\sigma_u$ level. However, we have no assurance that this last condition will be satisfied. The charge on the oxygen atom will probably decrease in order to compensate for the Coulomb repulsion between the negatively charged oxygen atoms. (Note that the charge on the silicon atoms decreased by a factor of 2 in going from SiO to Si_2O.) It is likely that more of this will come from the $2\pi_u$ orbital than from the $4\sigma_u$ orbital. Faced with these uncertainties, the matter of both the sign and magnitude of the correction due to more distant neighbors must be left open until SCF calculations on larger fragments are available.

The interpretation of the results of calculations with larger fragments will require some care. The additional oxygen atoms will not be at equivalent positions (i.e., in the same environment[39]). This can introduce spurious effects which are analogous to surface effects. In an Si_2O_7 fragment there will be one interior oxygen atom and six oxygen atoms on the surface. One should, therefore, use the separation of the levels in which the predominant atomic component is that of the central atom (or for which the admixtures of surface atom components have the same signature and comparable magnitudes) in order to determine the separation of the peaks in the emission spectrum. The distribution of the additional oxygen levels in Si_2O_7 would not provide a reliable picture of that part of the line broadening in silica which is due to the band structure of the electronic energy levels.

The spurious surface effects can be eliminated only by going to a much larger fragment, which is not feasible, or, for crystalline silica, by calculating MO's for the entire crystal. If one neglected all short-range interactions beyond second neighbors (exchange, overlap, etc.) and took the long-range Coulomb interactions into account by means of a point-ion field, then such a calculation would not be much more difficult than a calculation of the MO's for an Si_2O_7 fragment. However, it would be essential to take into account the modifications of the atomic orbitals. We have seen that the modifications of the orbitals which occur in going from an LCAO to an SCF calculation are important, so that an LCAO calculation would be a backward step.

A conventional SCF-MO calculation for a crystal presents computational problems associated with the fact that the modified atomic orbitals obtained by a population analysis are different for each level, and the number of levels in a crystal is infinite. The important distortions which occur can be expected to be due to the influence of near neighbors, so that it should be possible to take them into account in a crystal by doing an LCAO calculation with a small set of distorted atomic orbitals (DAO's) rather than by using the infinite set of MAO's obtained from a population analysis of the SCF-MO's. This approach may be implemented by transforming the Hartree-Fock equations to equations for localized orbitals.[40] The transformed equations appear as equations for individual atoms (or fragments) with additional terms which are due to the environment of neighboring atoms. The environmental terms may be treated in various approximations in order to obtain the distortion introduced by the environment to various levels of accuracy. The SCF solutions of the transformed equations are DAO's. The MO's are constructed as linear combinations of the DAO's so that the MO's and energy levels may be obtained by a linear-combination-of-distorted-atomic-orbitals (LCDAO) calculation which is entirely analogous to an LCAO calculation. The DAO's differ from the MAO's in that they do not depend on the molecular energy level. If the environmental terms were neglected entirely, the localized orbital equations for DAO's would reduce to the Hartree-Fock equations for isolated atoms, and the calculation would reduce to a conventional LCAO calculation. This localized orbital approach to the SCF problem for crystals has been applied to a number of different crystals by Kunz.[41]

When *ab initio* calculations are extended to fragments as large as Si_2O_7, it will be interesting to carry through a corresponding analysis of the silicon $K\beta$ and L emission spectra using the sequence of fragments Si, SiO_4, and Si_5O_4.

C. Electronic Correlation

The contribution associated with electronic correlation is generally understood to be the difference between an observable calculated in the Hartree-Fock (single-configuration) approximation and the same observable calculated by solving the nonrelativistic Schrödinger equation exactly. Relativistic effects and effects associated with the motion of the nuclei are regarded as separate contributions. The fixed-orbital approximation is also normally used for single-configuration calculations of excitation spectra. According to this convention, we have already included the most important electronic correlation effect by using the RO approximation in the single-configuration calculations for the collinear Si_2O fragment.

Calculations of the term splittings in isolated atoms have shown that correlation effects due to mixing of other configurations can have an important effect on the term separation.[42] The oscillator strengths are particularly sensitive to electronic correlation.[43] There are many ways of calculating this contribution. Perturbation calculations provide the most accurate results for isolated atoms, but are difficult to apply to molecules.[44,45] Other methods which show considerable promise include the many-electron theory of Sinanoğlu,[45] the Bethe-Goldstone method of Nesbet,[46] and the natural-orbital configuration-interaction method of Bender and Davidson.[47] We are inclined to favor the multiconfiguration SCF method, which is a direct extension of the Hartree-Fock approximation, and leads to a very compact and easily interpreted form for the wave function.[48] It has been applied with considerable success to both atoms and small molecules.

Electronic correlation will almost certainly be important for the oscillator strengths. In general, the correlation correction tends to decrease the oscillator strength for transitions in which the active electron remains in the same shell.[43] The effect may be reversed (and smaller) for intershell transitions due to a possible slight contraction of the charge distribution. The correlation corrections to the line positions are rather subtle, and there does not appear to be any reliable way to estimate their sign or magnitude from simple arguments.

VI. CONCLUSIONS

The calculations presented herein confirm the widely accepted interpretation of the origin of the primary and satellite peaks in the oxygen $K\alpha$ soft-x-ray emission spectrum of silica: the primary peak is due to electrons in levels which are of predominantly $2p\pi$(O) character dropping down to unoccupied $1s$(O) levels, while the low-energy satellite is due to electrons in levels which are of predominantly $2p\sigma$(O) character dropping down to unoccupied $1s$(O) levels. (π and σ orbitals are here defined as p orbitals which are parallel and perpendicular, respectively, to the plane which bisects the Si-O-Si angle.) The agreement between the experimental separation of 5 eV and the calculated separations of 4.4 eV for SiO, 6 eV for collinear Si_2O in the FO approximation, and 6.9 eV for collinear Si_2O in the RO approximation is not very good, but a qualitative analysis of the contributions from bending suggests that this correction would reduce the error, so that there is reason to expect that a more sophisticated calculation would yield good agreement. The 0.06% difference between the observed position of the primary line and the calculated position for Si_2O in the RO approximation provides more convincing quantitative evidence, even though the unusually good agreement is probably fortuitous.

These results were not unexpected. They serve primarily as a benchmark to show where we stand with regard to accurate interpretive and predictive calculations of the electronic energy levels and structure pertaining to soft-x-ray emission spectra. The more interesting results come from the additional information which one can extract from the *ab initio* wave functions. One bit of information was a more detailed explanation of the experimental fact that an oxygen $2s$(O) line is observed in the silicon $K\beta$ spectrum but not in the oxygen $K\alpha$ spectrum. Part of the explanation was well known and relatively trivial: The local symmetry is different for oxygen and silicon atoms, and the differences are such that a transition from the $2s$(O) level is forbidden for oxygen but allowed for silicon. The interesting and unexpected aspect was that crossover transitions in the literal sense of the word are very improbable: The $2s$(O)$\rightarrow 1s$)Si) transition is really a $3p'$(Si)$\rightarrow 1s$(Si) transition which occurs because there is an appreciable admixture of a modified $3p$(Si) atomic component in the t_2 orbital of SiO_4. Another interesting result was the strong enhancement of the oscillator strength due to contraction of the MAO components of the molecular orbitals. This result leads us to conclude that the LCAO approximation is inadequate for a quantitative, or even semiquantitative, interpretation of soft-x-ray emission spectra. One must use atomic orbitals obtained from SCF calculations.

The qualitative analysis of bending effects suggested that the shoulder observed on the low-energy side of the primary peak is due to splitting of the $2\pi_u$ level of the collinear Si_2O fragment, but SCF calculations for a bent fragment will be needed to verify this hypothesis.

The level of accuracy of both measurements and calculations is still much too low to permit one to infer bond angles from x-ray emission spectra.

However, if the resolution of the measurements could be improved by an order of magnitude, e.g., from the order of 0.5 to 0.05 eV, and accurate calculations embodying the refinements discussed in Sec. V were carried out, one might be able to extract information on the Si-O-Si bond angle.

The full value of the experimental data will be realized when the complete spectrum is calculated so that the information contained in the width of the emission bands can be extracted. This will require a calculation of the MO's and electronic energy bands for the entire crystal, and also a calculation of the interatomic forces and the Franck-Condon factors. A calculation at this level of sophistication would be an ambitious undertaking, but not beyond the realm of feasibility. The benefit would be that, in addition to providing a full interpretation of the emission spectrum, it would provide wave functions and energy levels that gave a rather complete characterization of the system and could be used for interpreting other experimental observations as well. The full wave function would also be useful as a starting point for studying the defect properties of silica.

ACKNOWLEDGMENTS

We acknowledge, with thanks, helpful correspondence from Professor W. Beall Fowler and Dr. D. S. Urch, an advance copy from Professor D. W. J. Cruickshank of his work on the silicate ion, and helpful conversations with Dr. William Primak on the properties of silica.

APPENDIX: MODIFIED ATOMIC ORBITALS AND ATOMIC POPULATIONS

Atomic population analysis, introduced by Mulliken in 1955,[49] is a familiar technique for analyzing MO's in terms of their atomic constituents. It is usually described in terms of the overlap matrix. In this work the emphasis is on the constituent atomic orbitals, which have been named modified atomic orbitals by Mulliken.[50] Since the analysis needed for this work is short and straightforward, but buried within other material in the literature in a variety of notations, a brief summary of the algorithms for constructing MAO's and calculating atomic populations is included in this appendix.

Molecular orbitals calculated in the SCF approximation by the Roothaan-expansion method (SCF-MO's) are represented by an expansion of the form

$$\psi_{i\lambda\alpha}(\vec{r}) = \sum_{\rho} C_{i\lambda\rho}\chi_{\rho\lambda\alpha}(\vec{r}) , \tag{A1}$$

where i is the principal index, λ and α are the MO symmetry indices, and ρ labels different basis functions of the same molecular symmetry. In a collinear molecule, $\rho = Alp$ represents three indices: an atomic site label, A = Si or O in the problem at hand; an atomic symmetry label; $l = 0, 1, 2, \ldots$ (or s, p, d, ...); and a label p for different atomic basis functions of the same symmetry on the same site. (In noncollinear molecules, the atomic symmetry index m must also be included, but for collinear molecules m is a unique function of λ and α.) The basis functions have the form

$$\chi_{\rho\lambda\alpha}(\vec{r}) = \chi_{Alp,\lambda\alpha}(r_A, \theta_A, \varphi_A) = R_{lp}(r_A)Y_{lm_{\lambda\alpha}}(\theta_A, \varphi_A) , \tag{A2}$$

where

$$R_{lp}(r) = [(2n_{lp})!\,]^{-1/2}(2\zeta_{lp})^{n_{lp}+1/2} \times r^{n_{lp}-1}e^{-\zeta_{lp}r} \tag{A3}$$

is a normalized Slater-type orbital which is completely characterized by two parameters, n_{lp} and ζ_{lp}, and $Y_{lm}(\theta, \varphi)$ is a spherical harmonic. The radial functions R_{lp} will be different for different atoms and may be different for different molecular symmetries, so that we should write $R_{lp}^{\lambda A}$ for a fully explicit notation, but we will omit the superscripts on R_{lp} in order to avoid a too confusing array of indices.

We may rewrite Eq. (5) as the sum

$$\psi_{i\lambda}(\vec{r}) = \sum_{Al} B_{i\lambda,Al}\,\varphi_{nl(A)}^{i\lambda}(\vec{r}) , \tag{A4}$$

where

$$\varphi_{nl(A)}^{i\lambda} \equiv r_A^{-1}P_{Al}^{i\lambda}(r)\,Y_{lm_{\lambda\alpha}}(\theta_A, \varphi_A) \tag{A5}$$

are MAO's which are constructed by summing over basis functions of the same atomic symmetry on the same site and renormalizing. The molecular and atomic symmetry subindices α and $m_{\lambda\alpha}$ have been omitted because they do not play a role in the analysis for collinear molecules. We have also added a principal atomic quantum index n in order to indicate the correspondence between the modified and unmodified AO's. (A principal atomic index is not essential because an MO can have only one atomic component for each atomic symmetry and site.) The unmodified AO's, $\varphi_{nl(A)}$, are identified by the absence of MO superscripts. [The notation $|nl^{i\lambda}(A)\rangle\rangle$ and $|nl(A)\rangle\rangle$ will also be used for MAO's and AO's, respectively.]

The expansion coefficients in Eq. (A4) are given by

$$B_{i\lambda,Al} = \{\int_0^\infty [\hat{P}_{Al}^{i\lambda}(r)]^2\,dr\}^{1/2} , \tag{A6}$$

where

$$\hat{P}_{Al}^{i\lambda}(r) = r\sum_{p} C_{i\lambda,Alp}\,R_{lp}(r) \tag{A7}$$

is the unnormalized radial MAO, obtained from Eqs. (A1) and (A2). The normalized radial MAO is

$$P_{Al}^{i\lambda}(r) = r\sum_{p} C'_{i\lambda,Alp}\,R_{lp}(r) , \tag{A8}$$

where $C'_{i\lambda,Alp} = C_{i\lambda,Alp}/B_{i\lambda,Al}$.

If we were to replace the MAO's by the unmodified AO's of the free atoms, we would obtain an LCAO rather than an SCF approximation. The modifications of the radial orbitals can be described roughly as a contraction or dilation, although more subtle changes in shape will also occur. The modifications will, of course, be different for different MO's, so that each MAO must be labeled by the MO indices $i\lambda$.

The atomic populations may be obtained directly from Eq. (A4). The net atomic population for the Ath atomic site and lth atomic symmetry type of the $i\lambda$th molecular level is $N_{i\lambda}|B_{i\lambda,Al}|^2$, where $N_{i\lambda}$ is the occupation of the $i\lambda$th molecular level. The gross atomic population is given by

$$N_{Al}^{i\lambda} = N_{i\lambda} \sum_{A'l'} B^*_{i\lambda,Al} \langle nl^{i\lambda}(A) | n'l'^{i\lambda}(A') \rangle B_{i\lambda,A'l'} \ . \quad \text{(A9)}$$

This definition is chosen in such a manner that the overlap charge is distributed between the overlapping atoms and the total charge in each shell is properly accounted for; thus,

$$\sum_{Al} N_{Al}^{i\lambda} = N_{i\lambda} \ . \quad \text{(A10)}$$

The ionic charge for a given species is defined to be

$$Q_A = \sum_{i\lambda l} N_{Al}^{i\lambda} - Z_A \ , \quad \text{(A11)}$$

where Z_A is the charge on the nucleus.

---

*Work performed under the auspices of the U.S. Atomic Energy Commission.

†NSF Postdoctoral Fellow.

‡Present address: University of Munich, West Germany.

[1]D. W. Fischer, J. Chem. Phys. **42**, 3814 (1965).

[2]G. Klein and H.-U. Chun, Phys. Status Solidi B **49**, 167 (1972).

[3]R. A. Mattson and R. C. Ehlert, Adv. X-Ray Anal. **9**, 471 (1966).

[4]The strong dependence of the high-energy oxygen $K\alpha$ satellites on the material used for the dispersing element was pointed out by Mattson and Ehlert (Ref. 3), and has also been noted by D. W. Fischer [J. Appl. Phys. **40**, 4151 (1969)] and discussed by Koster (Ref. 17). The origin of this effect is not yet fully understood. Fischer (Ref. 1) used a rubidium acid phthalate (RbAP) dispersing element; Mattson and Ehlert (Ref. 3) used a KAP dispersing element for SiO_2 (MgO and Al_2O_3 were studied with several different dispersing element materials); Ershov and Lukirskii (Ref. 5) used a gold-plated diffraction grating; and Klein and Chun (Ref. 2) use a concave grating of unspecified composition. Mattson and Ehlert also observed that the line at 532 eV decreases in intensity by about 25% in going from electron to x-ray excitation, and that the line at 538 eV disappears entirely for x-ray excitation.

[5]O. A. Ershov and A. P. Lukirskii, Fiz. Tverd. Tela **8**, 2137 (1966) [Sov. Phys.-Solid State **8**, 1699 (1967)].

[6]D. W. Fischer, Adv. X-Ray Anal. **13**, 159 (1970).

[7]K. Siegbahn *et al.*, *ESCA, Atomic Molecular and Solid State Structure Studied by Means of Electron Spectroscopy*, (Almqvist and Wiksells, Uppsala, 1967). (Electron spectroscopy for chemical applications is abbreviated ESCA.)

[8]T. H. DiStefano and D. E. Eastman, Phys. Rev. Lett. **27**, 1560 (1971).

[9]Ralph W. G. Wyckoff, *Crystal Structures* (Interscience, New York, 1963), Vol. 1; L. Bragg, G. F. Claringbull, and W. H. Taylor, *Crystal Structures of Minerals* (Cornell U. P., Ithaca, N. Y., 1965), *International Tables for X-Ray Crystallography*, edited by C. H. MacGillaury, G. D. Reick, and K. Lonsdale (Kynoch, Birmingham, England, 1968), Vol. III; A. G. Revesz, Phys. Rev. Lett. 27, 1578 (1971).

[10]R. L. Mozzi and B. E. Warren, J. Appl. Crystallogr. **2**, 164 (1969).

[11]D. S. Urch, J. Phys. C **3**, 1275 (1970). There are a few misprints and minor errors in this article which the author kindly pointed out to us.

[12]M. H. Reilly, J. Phys. Chem. Solids **31**, 1041 (1970).

[13]A. J. Bennett and L. M. Roth, J. Phys. Chem. Solids **32**, 1251 (1971).

[14]G. A. D. Collins, D. W. J. Cruickshank, and A. Breeze, J. C. S. Faraday II **1**, 1189 (1972).

[15]D. W. Fischer, J. Phys. Chem. Solids **32**, 2455 (1971); J. Appl. Phys. **41**, 3561 (1970). (This last reference only discusses the MO interpretation of the data, but includes a list of experimental references.)

[16]G. L. Glen and C. G. Dodd, J. Appl. Phys. **39**, 5372 (1968); C. G. Dodd and G. L. Glen, J. Appl. Phys. **39**, 5377 (1968); J. Appl. Phys. **40**, 2362(E) (1969); Am. Mineral. **54**, 1299 (1969); Am. Mineral. **55**, 1066(E) (1970); J. Am. Ceram. Soc. **53**, 322 (1970).

[17]A. S. Koster, Appl. Phys. Lett. **18**, 170 (1971); J. Phys. Chem. Solids **32**, 2685 (1971).

[18]A. R. Ruffa, Phys. Status Solidi **29**, 605 (1968); J. Appl. Phys. **43**, 4263 (1972).

[19]D. J. Nagel, Adv. X-Ray Anal. **13**, 182 (1970).

[20]W. L. Baun and D. W. Fischer, in *Spectroscopy in Inorganic Chemistry*, edited by C. N. R. Rao and J. R. Ferraro (Academic, New York, 1970), Vol. I, p. 209.

[21]*Soft X-Ray Band Spectra and the Electronic Structure of Metals and Materials*, edited by D. J. Fabian (Academic, New York, 1968). (Proceedings of a conference held at the University of Strathclyde, Scotland, 1967.)

[22]The view that silica consists of small Si^{+4} ions and large O^{--} ions appears to be based on radii deduced from ionic refractivities. One can obtain ionic refractivities by the application of additivity rules to the measured indices of refraction for a variety of crystals. The ionic radius may then be obtained from the ionic refractivity. [For a discussion of this approach and a bibliography of the original references see: J. H. Van Vleck, *The Theory of Electric and Magnetic Susceptibilities* (Oxford U. P., London, 1932), Sec. 52; J. R. Partington, *An Advanced Treatise on Physical Chemistry*, (Longmans, London, 1953), Vol. 4, pp. 555–560.] The Si^{+4} O_2^{-2} ionic model is adopted in work on the atomic theory of photoelasticity [H. Mueller, Physics (N.Y.) **6**, 179 (1935); J. Am. Ceram. Soc. **21**, 27 (1938)]. See also, W. Primak, *The Compacted States of Vitreous Silica* (Gordon and Breach, New York, to be published).

[23]P. S. Bagus, T. L. Gilbert, and C. C. J. Roothaan, J. Chem. Phys. **56**, 5195 (1972).

[24]C. Froese Fischer, Atomic Data **4**, 301 (1972).

[25]L. Pauling, *The Nature of the Chemical Bond* (Cornell U.P., Ithaca, N.Y., 1960).

[26]C. C. J. Roothaan and P. S. Bagus, Methods Comput. Phys. **2**, 47 (1963).
[27]P. S. Bagus and H. F. Schaeffer, III, J. Chem. Phys. **56**, 224 (1972).
[28]The error is increased when a ^1D or ^1S parent state is used because the valence orbitals in these states are dilated relative to the ^3P valence orbitals. It is found that the calculated emission energies for ^1D and ^1S parent states are ~ 0.5–~ 1.0 eV larger than for a ^3P parent state.
[29]P. S. Bagus, Phys. Rev. **139**, A619 (1965).
[30]J. C. Slater, *Quantum Theory of Atomic Structure* (McGraw-Hill, New York, 1960), Vol. I, Chap. 15; see also, P. S. Bagus and C. M. Moser, Phys. Rev. **167**, 13 (1968); J. Phys. B **2**, 1214 (1969); P. S. Bagus, N. Bessis, and C. M. Moser, Phys. Rev. **179**, 39 (1969).
[31]The first equality may be obtained from the standard identities in the theory of angular momentum. See, for example, E. Feenberg and G. E. Pake, *Notes on the Quantum Theory of Angular Moment* (Stanford U. P., Palo Alto, Calif., 1969), p. 50. The second step may be obtained from the expansion of $\langle \alpha' L' M' |$ and $|\alpha L M\rangle$ into a sum of Slater determinants. See J. C. Slater, *Quantum Theory of Atomic Structure* (McGraw-Hill, New York, 1960), Vol. II.
[32]P. S. Bagus, *SCF Excited States and Transition Probabilities of Some Neon-Like and Argon-Like Ions*, Argonne National Laboratory Report No. ANL-6959, 1964. (Available from the Clearinghouse for Federal Scientific and Technical Information, National Bureau of Standards, U. S. Dept. of Commerce, Springfield, Va.).
[33]The internuclear distance for silica is R = 3.06 B (1.62 Å) but the values of ΔE for the three valence levels at this distance do not differ from those at $R = 3.104\,B$ by more than $0.004\,H$ (0.1 eV). The value of ΔE for the 5σ level is about 0.2 eV less at $R = 3.06\,B$.
[34]A. D. McLean and M. Yoshimine, *Tables of Linear Molecule Wave Functions*, IBM J. Res. Dev., November 1967.
[35]A. C. Wahl, P. J. Bertoncini, G. Das, and T. L. Gilbert, Int. J. Quantum Chem. Symp. **1S**, 123 (1967).
[36]H. M. O'Bryan and H. W. B. Skinner, Proc. R. Soc. A **176**, 229 (1940). See also Ref. 11, and W. L. Baun and D. W. Fischer, Spectrochim. Acta **21**, 1471 (1965).
[37]The ALCHEMY program has been designed and coded by P. S. Bagus, M. Yoshimine, A. D. McLean, and B. Liu. The program calculates self-consistent-field molecular orbitals by means of the Roothaan-expansion method in both the single-configuration (Hartree-Fock) and multiconfiguration approximations. A description of the program and its capabilities may be found in *Proceedings of the Conference on Potential Energy Surfaces in Chemistry*, edited by W. A. Lester, Jr., which is available as publication RA 18, January 14, 1971 (No. 14748) from the Research Library, IBM Research Laboratory, Monterey and Cottle Roads, San Jose, Calif. 95114.
[38]For a copy of these listings, order NAPS Document No. 02237 from ASIS National Auxiliary Publications Service, c/o Information Corp., 866 Third Avenue, New York, N. Y., 10022; remitting $1.50 for microfiche or $9.80 for photocopies.
[39]A unit lattice cell in crystalline quartz contains three silicon atoms and six oxygen atoms, so that only one out of every six oxygens are equivalent in the usual sense; i.e., with respect to total environment. There are small changes in the Si-O-Si bond angle, and, if next-nearest neighbors are considered, small differences can appear because the plane of the bent Si-O-Si fragment may be differently oriented with respect to triangular bases of the tetrahedrons in the bipyramidal Si_2O_7 structure. The environmental differences between inequivalent oxygen atoms in silica will be much smaller than the environmental differences between oxygen atoms on the "surface" and interior of an Si_2O_7 fragment.
[40]T. L. Gilbert, Phys. Rev. A **6**, 580 (1972).
[41]A. B. Kunz, J. Phys. C **3**, 1542 (1970); Phys. Rev. B **4**, 609 (1971); Phys. Status Solidi B **46**, 385 (1971); Phys. Status Solidi B **46**, 697 (1971); N. O. Lipari and A. B. Kunz, Phys. Rev. B **4**, 4639 (1971).
[42]P. S. Bagus and C. M. Moser, Phys. Rev. **167**, 13 (1968); J. Phys. B **2**, 1214 (1969); P. S. Bagus, N. Bessis, and C. M. Moser, Phys. Rev. **179**, 39 (1969).
[43]O. Sinanoğlu, Comments At. Mol. Phys. **2**, 73 (1970).
[44]H. P. Kelly, Adv. Chem. Phys. **14**, 129 (1969).
[45]O. Sinanoğlu and K. A. Brueckner, *Three Approaches to Electron Correlation in Atoms* (Yale U. P., New Haven, Conn., 1970).
[46]R. K. Nesbet, Phys. Rev. **155**, 51 (1967); Phys. Rev. **155**, 56 (1967); Phys. Rev. **175**, 2 (1968).
[47]C. F. Bender and E. R. Davidson, J. Chem. Phys. **47**, 360 (1967); Phys. Rev. **183**, 23 (1969).
[48]See Refs. 19–36 cited in Ref. 40.
[49]R. S. Mulliken, J. Chem. Phys. **23**, 1833 (1955).
[50]R. S. Mulliken, J. Chem. Phys. **36**, 3428 (1962).